

DOMINION NA 3 IN-PROCESS STATUS FORM	
Document Title	Benchmarking of SASSI2010 MSM Results from NA3 Site-Specific SSI Analysis
Document Type	Shimizu Engineering Report
Revision ID (if applicable)	SER-DMN-011, Rev. 1 (in Shimizu's doc. number)
Author / Responsible Engineer	R. Ikeda, Shimizu Corporation
Lead	R. Ikeda, Shimizu Corporation
Date (Last Update/Revision)	7/10/15
Document/Work Status e.g. Pending, Active, On-hold, Complete-In Verification, Verified-Waiting eCM	Issued for Use Verification has been performed (ES1505-V07).
Specific Cautions To Users e.g. Enumerate/list specific incomplete content. Enumerate/list specific complete but unverified content. Enumerate/list key areas of technical uncertainty and parameters impacted.	<p>This report documents the benchmarking of SASSI2010 Modified Subtraction Method (MSM) for the North Anna Unit 3 (NA3) site-specific SSI and SSSI analyses for Dominion NA 3 ESBWR project.</p> <p>The analysis conditions are provided by the following Design Inputs:</p> <ul style="list-style-type: none"> 105E3908 , Revision 5 105E4483 , Revision 1 26A6642AL, Revision 10 26A6647, Revision 7 26A6648, Revision 4 26A7419, Revision 1 TODI WG3-3-A25-TDI-0005, Revision 5 TODI WG3-3-A25-TDI-0006, Revision 0 TODI-WG3-A25-TDI-S-0004, Revision 0 <p>This report is revised to incorporate the GEH comments on the previous report which are e-mailed from Ms. Tanya Kirby titled "RE: MSM eigenvalue analyses preliminary results", dated July 8, 2015.</p>
Cross-reference Information e.g. eDRF or other useful data pointers	

Shimizu Engineering Report

Project	GE-Hitachi Nuclear Energy Dominion NA3 ESBWR Project	Shimizu Document No.	SER-DMN-011
Title	Benchmarking of SASSI2010 MSM Results from NA3 Site-Specific SSI Analysis	Rev.	1
		Issued Date	7/14/14
		Revised Date	7/10/15

NOTE:

This report documents the benchmarking of SASSI2010 Modified Subtraction Method (MSM) for the North Anna Unit 3 (NA3) site-specific SSI and SSSI analyses. The benchmarking is based on the results of SSI analyses of NA3 FWSC model and the benchmarking analyses performed on the Enrico Fermi Unit 3 (EF3) RB/FB, CB and FWSC models. ANSYS eigenvalue analyses are performed on RB/FB, CB, FWSC, CB-FWSC, CB-RB/FB and FWSC-CB excavated volume models with properties representing the corresponding NA3 full column subgrade profiles that include the soil above the rock. The results of these eigenvalue analyses indicate that among the six NA3 models, the FWSC model is prone to errors due to the MSM approximation. The comparison of results obtained from SASSI 2010 analyses of NA3 FWSC model obtained using the MSM and the explicit Direct Method (DM) show negligible differences between the two solutions. A comprehensive study of the NA3 and the EF3 subgrade conditions demonstrates the applicability of the results of the EF3 benchmarking analyses for the NA3 site.

The input for the analysis presented in this report are obtained from the following sources:


105E3908 , Revision 5	
105E4483 , Revision 1	TODI WG3-3-A25-TDI-0005, Revision 5
26A6642AL, Revision 10	TODI WG3-3-A25-TDI-0006, Revision 0
26A6647, Revision 7	TODI WG3-A25-TDI-S-0004, Revision 0
26A6648, Revision 4	
26A7419, Revision 1	

SASSI version 2010 was obtained from Isatis LLC under the contract with the Regents of the University of California and implemented by Shimizu Corporation of Tokyo, Japan on HP Z420 Workstation computer using Windows 7 OS. Program validation documentation is available at Shimizu Corporation.

IMPORTANT NOTICE REGARDING CONTENTS OF THIS REPORT
Please Read Carefully

The design, engineering, and other information contained in this document are furnished in accordance with the Development Agreement between Virginia Electric and Power Company and the Consortium of GE-Hitachi Nuclear Energy Americas LLC and Fluor Enterprises, Inc. dated April 5, 2013 as amended. Nothing contained in this document shall be construed as changing the Contract. The use of this information by anyone other than Virginia Electric and Power Company, or for any purpose other than that for which it is furnished by GEH is not authorized; and with respect to any unauthorized use, GEH makes no representation or warranty, express or implied, and assumes no liability as to the completeness, accuracy, or usefulness of the information contained in this document, or that its use may not infringe privately owned rights.

Copyright 2015 GE-Hitachi Nuclear Energy Americas LLC, All Rights Reserved

1	7/10/15	Issue for Use	Y. O.	S. O.	R. I.
0	7/14/14	Issue for Use	Y. O.	S. O.	R. I.
Rev.	Date	Note	Approve	Review	Prepare
			Prepared by	R. Ikeda	7/14/14
			Reviewed by	S. Oguri	7/14/14
			Approved by	Y. Orito	7/14/14

**TABLE OF CONTENTS**

1.	INTRODUCTION AND PURPOSE	7
2.	REFERENCES	8
3.	EIGENVALUE ANALYSES OF EXCAVATED VOLUME MODELS	8
3.1	RB/FB Excavated Volume Eigenvalue Analysis.....	9
3.1.1	Analysis Model	9
3.1.2	Results	10
3.2	CB Excavated Volume Model Eigenvalue Analysis	10
3.2.1	Analysis Model	10
3.2.2	Results	10
3.3	FWSC Excavated Volume Model Eigenvalue Analysis.....	11
3.3.1	Analysis Model	11
3.3.2	Results	11
4.	FWSC BENCHMARKING ANALYSIS	11
4.1	DM Analysis Model.....	11
4.2	Results.....	12
4.2.1	Comparison of Transfer Functions	12
4.2.2	Comparison of ISRS	12
4.2.3	Comparison of Maximum Absolute Accelerations.....	12
4.2.4	Comparison of Maximum Forces and Moments	13
4.2.5	Comparison of Maximum Relative Displacements	13
5.	EF3 MSM BENCHMARKING EVALUATION	13
5.1	Results of EF3 Benchmarking Analyses.....	13
5.2	Comparisons of EF3 and NA3 Subgrade Conditions	14
5.3	Applicability of EF3 MSM Benchmarking Analyses Results for NA3 Site	15
6.	CONCLUSIONS.....	15



LIST OF TABLES

Table 3-1	Boundary Conditions of Half Models for Excavated Volume	17
Table 3.1-1	UB Soil Layers Properties of RB/FB Excavated Volume Model	18
Table 3.1-2	The Ratio of Layer Thickness to the Shortest Shear Wave Length for RB/FB	18
Table 3.1-3	Location of Interaction Nodes within RB/FB Excavated Volume	19
Table 3.1-4	Natural Frequencies of RB/FB Excavated Volume Model	19
Table 3.2-1	UB Soil Layers Properties of CB Excavated Volume Model	20
Table 3.2-2	The Ratio of Layer Thickness to the Shortest Shear Wave Length for CB	21
Table 3.2-3	Location of Interaction Nodes within CB Excavated Volume	24
Table 3.2-4	Traveling Times of Shear Wave for CB Excavated Volume	24
Table 3.2-5	Natural Frequencies of CB Excavated Volume Model	25
Table 3.3-1	UB Soil Layers Properties of FWSC Excavated Volume Model	26
Table 3.3-2	The Ratio of Layer Thickness to the Shortest Shear Wave Length for FWSC	27
Table 3.3-3	Location of Interaction Nodes within FWSC Excavated Volume	29
Table 3.3-4	Traveling Times of Shear Wave for FWSC Excavated Volume	29
Table 3.3-5	Natural Frequencies of FWSC Excavated Volume Model	30
Table 4-1	Summary of Excavated Volumes Eigenvalue Analyses Results	31
Table 4.1-1a	Location of Interaction Nodes within FWSC Excavated Volume at Upper Bound Subsurface Profiles	32
Table 4.1-1b	Location of Interaction Nodes within FWSC Excavated Volume at Lower Bound Subsurface Profiles	32
Table 4.2-1a	Comparison of FWSC Maximum Absolute Accelerations from UB Subgrade Profile Analyses	33
Table 4.2-1b	Comparison of FWSC Maximum Absolute Accelerations from LB Subgrade Profile Analyses	34
Table 4.2-2a	Comparison of FWSC Maximum Response Forces and Moments from UB Subgrade Profile Analyses	35
Table 4.2-2b	Comparison of FWSC Maximum Response Forces and Moments from LB Subgrade Profile Analyses	36
Table 4.2-3a	Comparison of FWSC Maximum Relative Displacement from UB Subgrade Profile Analyses	37
Table 4.2-3b	Comparison of FWSC Maximum Relative Displacement from LB Subgrade Profile Analyses	38
Table 5.2-1	Properties of RB/FB and CB Embedment at NA3 and EF3 Sites	39



LIST OF FIGURES

Figure 3.1-1	Soil Layers of RB/FB Excavated Volume Model.....	40
Figure 3.1-2	RB/FB Excavated Volume Mode Shapes	41
Figure 3.2-1	Soil Layers of CB Standalone Excavated Volume Model	42
Figure 3.2-2	Soil Layers of CB-FWSC Combined Excavated Volume Half Model.....	43
Figure 3.2-3	Soil Layers of CB-RB/FB Combined Excavated Volume Model	44
Figure 3.2-4	CB Standalone Excavated Volume Mode Shapes	45
Figure 3.2-5	CB Excavated Volume Mode Shapes for CB-FWSC Combined Model	46
Figure 3.2-6	CB Excavated Volume Mode Shapes for CB-RB/FB Combined Model	47
Figure 3.3-1	Soil Layers of FWSC Standalone Excavated Volume Half Model	48
Figure 3.3-2	Soil Layers of FWSC-CB Combined Excavated Volume Half Model.....	49
Figure 3.3-3	FWSC Standalone Excavated Volume Mode Shapes.....	50
Figure 3.3-4	FWSC Excavated Volume Mode Shapes for FWSC-CB Combined Model	51
Figure 4.1-1	DM Analysis Model for FWSC	52
Figure 4.1-2	FWSC Seismic Analysis Stick Model.....	53
Figure 4.2-1a	Comparison of Transfer Functions for FWS Wall Top Response - UB Subgrade Profile Analysis.....	54
Figure 4.2-1b	Comparison of Transfer Functions for FWS Wall Top Response - LB Subgrade Profile Analysis.....	55
Figure 4.2-2a	Comparison of Transfer Functions for FWS Basemat Response - UB Subgrade Profile Analysis.....	56
Figure 4.2-2b	Comparison of Transfer Functions for FWS Basemat Response - LB Subgrade Profile Analysis.....	57
Figure 4.2-3a	Comparison of Transfer Functions for FPE Top Response - UB Subgrade Profile Analysis.....	58
Figure 4.2-3b	Comparison of Transfer Functions for FPE Top Response - LB Subgrade Profile Analysis.....	59
Figure 4.2-4a	Comparison of Transfer Functions for FPE Basemat Response - UB Subgrade Profile Analysis.....	60
Figure 4.2-4b	Comparison of Transfer Functions for FPE Basemat - LB Subgrade Profile Analysis.....	61
Figure 4.2-5a	Comparison of ISRS for FWS Top Response in X-direction from UB Subgrade Profile Analysis.....	62
Figure 4.2-5b	Comparison of ISRS for FWS Top Response in X-direction from LB Subgrade Profile Analysis.....	62
Figure 4.2-6a	Comparison of ISRS for FWS Basemat Response in X-direction from UB Subgrade Profile Analysis.....	63
Figure 4.2-6b	Comparison of ISRS for FWS Basemat Response in X-direction from LB Subgrade Profile Analysis.....	63
Figure 4.2-7a	Comparison of ISRS for FPE Top Response in X-direction from UB Subgrade Profile Analysis.....	64



Figure 4.2-7b Comparison of ISRS for FPE Top Response in X-direction from LB Subgrade Profile Analysis.....	64
Figure 4.2-8a Comparison of ISRS for FPE Basemat Response in X-direction from UB Subgrade Profile Analysis.....	65
Figure 4.2-8b Comparison of ISRS for FPE Basemat Response in X-direction from LB Subgrade Profile Analysis.....	65
Figure 4.2-9a Comparison of ISRS for FWS Top Response in Y-direction from UB Subgrade Profile Analysis.....	66
Figure 4.2-9b Comparison of ISRS for FWS Top Response in Y-direction from LB Subgrade Profile Analysis.....	66
Figure 4.2-10a Comparison of ISRS for FWS Basemat Response in Y-direction from UB Subgrade Profile Analysis.....	67
Figure 4.2-10b Comparison of ISRS for FWS Basemat Response in Y-direction from LB Subgrade Profile Analysis.....	67
Figure 4.2-11a Comparison of ISRS for FPE Top Response in Y-direction from UB Subgrade Profile Analysis.....	68
Figure 4.2-11b Comparison of ISRS for FPE Top Response in Y-direction from LB Subgrade Profile Analysis.....	68
Figure 4.2-12a Comparison of ISRS for FPE Basemat Response in Y-direction from UB Subgrade Profile Analysis.....	69
Figure 4.2-12b Comparison of ISRS for FPE Basemat Response in Y-direction from LB Subgrade Profile Analysis.....	69
Figure 4.2-13a Comparison of ISRS for FWS Top Response in Z-direction from UB Subgrade Profile Analysis.....	70
Figure 4.2-13b Comparison of ISRS for FWS Top Response in Z-direction from LB Subgrade Profile Analysis.....	70
Figure 4.2-14a Comparison of ISRS for FWS Basemat Response in Z-direction from UB Subgrade Profile Analysis.....	71
Figure 4.2-14b Comparison of ISRS for FWS Basemat Response in Z-direction from LB Subgrade Profile Analysis.....	71
Figure 4.2-15a Comparison of ISRS for FPE Top Response in Z-direction from UB Subgrade Profile Analysis.....	72
Figure 4.2-15b Comparison of ISRS for FPE Top Response in Z-direction from LB Subgrade Profile Analysis.....	72
Figure 4.2-16a Comparison of ISRS for FPE Basemat Response in Z-direction from UB Subgrade Profile Analysis.....	73
Figure 4.2-16b Comparison of ISRS for FPE Basemat Response in Z-direction from LB Subgrade Profile Analysis.....	73
Figure 5.2-1 NA3 and EF3 S-wave and P-wave Velocity Profiles.....	74



LIST OF ACRONYMS

BE	Best Estimate
CB	Control Building
DM	Direct Method
EF3	Enrico Fermi Unit 3
FPE	Fire Pump Enclosure
FWS	Firewater Storage Tanks
FWSC	Firewater Service Complex
ISRS	In-Structure Response Spectra
MSM	Modified Subtraction Method
NA3	North Anna Unit 3
RB/FB	Reactor Building/Fuel Building
SSI	Soil-Structure Interaction
SSSI	Structure- Soil-Structure Interaction
UB	Upper Bound



1. INTRODUCTION AND PURPOSE

The North Anna Unit 3 (NA3) site-specific Soil-Structure Interaction (SSI) and Structure-Soil-Structure Interaction (SSSI) analyses of fully embedded models for frequencies up to 70 Hz, require refined models of the excavated volumes with a large number of nodes that exceeds the SASSI 2010 limitation on the maximum number ($< 20,000$) of interaction nodes for impedance calculations (Reference 2-d). Therefore, these analyses cannot be performed using the explicit Direct Method (DM) where all of the excavated volume nodes are specified as interaction nodes. Instead, the Modified Subtraction Method (MSM) is used for the NA3 SSI and SSSI analyses of fully embedded models in which only selected nodes of the excavated volume are specified as interaction nodes.

This report presents the benchmarking of the MSM for the NA3 site-specific SSI and SSSI analyses to demonstrate the accuracy of the SASSI 2010 solutions obtained based on this modeling approximation. The MSM benchmarking is based on the results of SSI analyses of the NA3 FWSC model and the results of the benchmarking analyses performed for the Enrico Fermi Unit 3 (EF3) RB/FB, CB, and FWSC models documented in References 2-e, 2-f, and 2-g, respectively. ANSYS eigenvalue analyses are also performed in Reference 2-j on excavated volume models with properties corresponding to the upper bound (UB) full column subgrade profiles that include the in-situ soil above the NA3 Zone III rock. Eigenvalue analyses are performed on the excavated volume models used for:

- RB/FB SSI analyses of full column profiles documented in Reference 2-a,
- CB SSI analyses of full column profiles documented in Reference 2-b,
- CB-RB/FB SSSI analyses of full column profile documented in Reference 2-i,
- FWSC SSI analyses documented in Reference 2-c,
- CB-FWSC and FWSC-CB SSSI analyses documented in Reference 2-h.

The results of the eigenvalue analyses indicate that among these models, the model used for the FWSC SSI analyses is the one that is prone to errors due to the MSM approximation. Therefore, an SASSI2010 MSM benchmarking analyses are performed for the upper bound (UB) and lower bound (LB) subgrade profiles using models that have the same configuration, meshing, and dynamic properties as the models used for the FWSC SSI analysis documented in Reference 2-c. The only difference between the two models is the number of interaction nodes. The accuracy of the MSM results is demonstrated by comparing the results for transfer functions, in-structure response spectra (ISRS), maximum absolute accelerations, maximum member forces, and maximum relative displacements from the FWSC licensing basis analysis documented in Reference 2-c that was performed using the MSM approximation with the corresponding results obtained using the explicit Direct Method (DM).



The results of the benchmarking analyses performed on the EF3 RB/FB and CB fully embedded models, that are documented in References 2-e and 2-f, are also used to demonstrate the adequacy of the MSM for the site-specific SSI analyses of the NA3 RB/FB and CB models. The results of a comprehensive study of the NA3 and EF3 subgrade conditions demonstrate the applicability of the results of these EF3 benchmarking analyses for the NA3 site.

2. REFERENCES

- a. WG3-U71-ERD-S-0001, North Anna 3 Reactor/Fuel Building Complex Seismic Analysis Report, Revision 1
- b. WG3-U73-ERD-S-0001, North Anna 3 Control Building Seismic Analysis Report, Revision 0
- c. WG3-U63-ERD-S-0001, North Anna 3 Firewater Service Complex Seismic Analysis Report, Revision 0.
- d. SASSI 2010 V&V Report, Shimizu Corporation, Revision H, June 26, 2015
- e. DTE Electric Company, Enrico Fermi Unit 3 – ESBWR, Sargent & Lundy Report SL-011814, Modified Subtraction Method (MSM) Reactor Building/Fuel Building Benchmark Summary Report, Revision 0, May 2, 2013 (NRC ADAMS Accession Number ML13127A034)
- f. DTE Electric Company, Enrico Fermi Unit 3 – ESBWR, Sargent & Lundy Report SL-011874, Modified Subtraction Method (MSM) Control Building Benchmark Summary Report, Revision 0, June 10, 2013 (NRC ADAMS Accession Number ML13175A263)
- g. DTE Electric Company, Enrico Fermi Unit 3 – ESBWR, Sargent & Lundy Report SL-011863, Modified Subtraction Method (MSM) Firewater Service Complex Benchmark Summary Report, Revision 0, May 21, 2013 (NRC ADAMS Accession Number ML13175A264)
- h. WG3-U73-ERD-S-0002, North Anna 3 Control Building and Fire Water Complex Seismic Structure-Soil-Structure Interaction Analysis Report, Revision 2
- i. WG3-U73-ERD-S-0005, North Anna 3 Control Building and Reactor/Fuel Building Complex Seismic Structure-Soil-Structure Interaction Analysis Report, Revision 0
- j. DBR-0010510, Natural Frequencies of the Excavated Volumes of RBFB, CB, CB-RBFB, CB-FWSC, FWSC and FWSC-CB Models for SSI and SSSI Analyses, Revision 0

3. EIGENVALUE ANALYSES OF EXCAVATED VOLUME MODELS

Although no explicit relationship can be established between the dynamic properties of the MSM excavated volume models and the accuracy of the MSM solutions, the higher values of the natural frequencies of vibration of the excavated volume that are closer to the frequency range of interest to the SSI and SSSI analyses indicate that the model will be less prone to errors due to the MSM modeling approximation.



In order to obtain the natural frequencies and modes of vibrations of the excavated volumes used for the NA3 SSI and SSSI analyses of full column profiles, ANSYS eigenvalue analyses are performed in Reference 2-j on the excavated volume models used for the NA3 site-specific SSI and SSSI analyses of UB full column subgrade profiles. Pinned boundary conditions are established at the location of the interaction nodes in the MSM models. The eigenvalue analyses are performed on full excavated volumes models used for the analyses of RB/FB and CB SSI and CB-RB/FB SSSI analyses of UB full column profiles. Half models with symmetry or asymmetry boundary conditions are used for the eigenvalue analyses of the excavated volume models used for the FWSC SSI, CB-FWSC SSSI and FWSC-CB SSSI analyses of UB subgrade profiles. The interaction nodes are defined at the following locations:

- at the bottom of the excavated volumes,
- at the vertical side surfaces of the excavated volume at the interfaces with the far-field model,
- at the ground surface,
- at additional horizontal planes within the excavated volume, and
- at additional vertical plane between two buildings within the excavated volume for combined models.

Symmetry and anti-symmetry boundary conditions are defined at the vertical planes of symmetry established at the middle of the FWSC standalone, CB-FWSC combined, and FWSC-CB combined half models. Table 3-1 presents the set of different boundary conditions established at the planes of symmetry in order to consider all possible modes of vibration of the excavated volume models.

The number of the additional horizontal planes of interaction nodes are identical to the SASSI models used for the seismic analyses in References 2-a, 2-b, 2-c, 2-h and 2-i. The locations of the additional horizontal planes of interaction nodes are determined based on equivalent shear wave arrival time calculations. These calculations help find the location of the additional horizontal planes of interaction nodes so the times of the waves travel through separated parts of the excavated volume are approximately equal.

3.1 RB/FB Excavated Volume Eigenvalue Analysis

3.1.1 Analysis Model

Figure 3.1-1 shows the RB/FB excavated soil volume model used for the eigenvalue analysis which is composed of five soil layers as shown in Table 3.1-1 with in-situ soil properties corresponding to those of the RB/FB UB full column profile used for the NA3 site-specific RB/FB SSI analysis. The configuration and mesh sizes of this excavated volume model are identical to the SASSI2010 excavated volume model used for the seismic analysis of the



RB/FB fully embedded model documented in Reference 2-a. The model is a full model without plane of symmetry. The ratio of layer thickness to the shortest shear wave length, considering 70Hz as the highest frequency of analyses, is shown in Table 3.1-2.

One horizontal plane of interaction nodes is defined within the excavated volume at EL 0.08 m. By using the equivalent traveling time method, the location of this plane of interaction nodes is calculated to be at EL -0.34 m as shown in Table 3.1-3. The actual plane of interaction nodes is established at the nearest horizontal node plane elevation located at EL 0.08 m. Figure 3.1-1 also presents the elevations of the horizontal planes of interaction nodes in the RB/FB excavated volume model.

3.1.2 Results

Table 3.1-4 presents a summary of results from the eigenvalue analyses of the RB/FB excavated volume models. Plots of the resulting mode shapes below 70 Hz from the analyses of each one of the excavated volume models are shown in Figure 3.1-2. The minimum natural frequency calculated for the RB/FB excavated volume model is 57.3 Hz.

3.2 CB Excavated Volume Model Eigenvalue Analysis

3.2.1 Analysis Model

Figures 3.2-1 through 3.2-3 show the CB standalone, CB-FWSC combined, and CB-RB/FB combined volume models of excavated soil used for the eigenvalue analysis. These models consist of six soil layers as shown in Table 3.2-1 with in-situ soil properties corresponding to those of the CB UB full column profile. The configuration mesh sizes and soil properties of these excavated volume models are identical to the SASSI2010 excavated volume models used for the CB SSI, CB-FWSC SSSI and CB-RB/FB SSSI analyses of the CB UB full column profile. The CB SSI standalone and CB-RB/FB SSSI combined models are full models without plane of symmetry. The CB-FWSC SSSI combined model is a half model with one vertical (YZ) plane of symmetry. The ratio of layer thickness to the shortest shear wave length, considering 70Hz as the highest frequency of analysis, is shown in Table 3.2-2.

Two horizontal planes of interaction nodes are defined within the excavated volumes of the CB SSI standalone, CB-FWSC SSSI combined, and CB-RB/FB SSSI combined models with elevations determined based on the equivalent shear wave traveling time calculations presented in Table 3.2-3. The analysis cases, locations of the interaction node planes, and traveling times of shear wave are summarized in Table 3.2-4 and the elevations of interaction node planes are shown in Figures 3.2-1 through 3.2-3 for each model.

3.2.2 Results

Table 3.2-5 presents a summary of results from the eigenvalue analyses of the excavated volume models used for the CB SSI, CB-FWSC SSSI and CB-RB/FB SSSI analyses. Plots of the resulting mode shapes below 70 Hz from the analyses of each one of the excavated volume models are shown in Figures 3.2-4 through 3.2-6. The minimum natural frequency



calculated for the three models are 57.7 Hz, 60.6 Hz, and 53.9 Hz for the CB SSI standalone, CB-FWSC SSSI combined, and CB-RB/FB SSSI combined models, respectively.

3.3 FWSC Excavated Volume Model Eigenvalue Analysis

3.3.1 Analysis Model

Figures 3.3-1 and 3.3-2 show the FWSC standalone and FWSC-CB combined models of excavated soil volume used for the eigenvalue analysis. These models consist of six soil layers as shown in Table 3.3-1 with in-situ soil properties corresponding to those of the FWSC UB profile. The configuration and mesh sizes of these excavated volume models are identical to the SASSI2010 excavated volume models used for the the FWSC SSI and the FWSC-CB SSSI analyses. These models are half models with one vertical (YZ) plane of symmetry. The ratios of layer thickness to the shortest shear wave length, considering 70Hz as the highest frequency, are shown in Table 3.3-2.

Two horizontal planes of interaction nodes are also defined within the excavated volume model with elevations determined based on the equivalent shear wave traveling time calculations presented in Table 3.3-3.

The analysis cases, locations of the interaction node planes and traveling times of shear wave are summarized in Table 3.3-4, and the elevations of interaction node planes are shown in Figures 3.3-1 and 3.3-2 for each model.

3.3.2 Results

Table 3.3-5 presents a summary of results from the eigenvalue analyses of the excavated volume models used for the FWSC SSI and FWSC-CB SSSI analyses. Plots of the resulting mode shapes below 70 Hz from the analyses of each one of the excavated volume models are shown in Figures 3.3-3 and 3.3-4. The minimum natural frequency calculated for the two models are 48.5 Hz and 42.8 Hz for the FWSC SSI standalone and FWSC-CB SSSI combined models, respectively.

4. FWSC BENCHMARKING ANALYSIS

The summary of the results of the eigenvalue analyses in Table 4-1 show that the natural frequencies of the FWSC SSI and FWSC-CB SSSI excavated volume models are less than 50 Hz. Since this is an indicator that the FWSC MSM model is the most prone to errors due to the MSM approximation, the focus of the NA3 SASSI2010 MSM benchmarking evaluation is on the FWSC excavated volume model.

4.1 DM Analysis Model

The configuration, properties, and mesh of the model used for the MSM benchmarking analysis are the same as those of the half model used for the licensing basis seismic analyses of the FWSC SSI in Reference 2-c for the UB and LB subgrade profiles. The only difference



is that the model used for the MSM benchmark analysis uses the explicit DM and has all nodes of excavated volume specified as interaction nodes, unlike the licensing basis model that uses the MSM approximation and has interaction nodes defined at seven planes of nodes located at:

- the bottom of the excavated volume at EL -16.84 m,
- the three vertical side surfaces of the excavated volume,
- the ground surface at EL 2.15 m, and
- the horizontal planes within the excavated volume at EL -1.60 m and EL -5.91 m.

Since the model used for the licensing basis seismic analyses in Reference 2-c represents half of the FWSC, interaction nodes are not defined at the YZ vertical plane of symmetry at the middle of the FWSC, except for the intersections between the four horizontal and two vertical planes of interaction nodes and the symmetry plane. The elevations of the horizontal planes of interaction nodes within the excavated volume are defined based on the equivalent traveling time of the FWSC in-situ soil profile as shown in Tables 4.1-1a and 4.1-1b for UB and LB subsurface profiles, respectively. Figures 4.1-1 and 4.1-2 present the FWSC model used for MSM benchmarking analysis.

The DM SSI analyses are performed for the same set of frequencies as the one used for the licensing basis analysis presented in Table 4.2-2 of Reference 2-c. The cut-off frequencies of the analyses of LB and UB subgrade profile are 36 Hz and 70 Hz, respectively.

4.2 Results

4.2.1 Comparison of Transfer Functions

Figures 4.2-1a through 4.2-4b show comparisons of transfer functions at key locations within the FWSC calculated using MSM and DM. The transfer functions obtained from the MSM analyses are almost identical to those obtained from the DM analysis.

4.2.2 Comparison of ISRS

Figures 4.2-5a through 4.2-16b show comparisons of the MSM and DM analyses results for 5% damped ISRS at key locations within the FWSC. The comparisons demonstrate that the ISRS results from the MSM and DM analyses are virtually identical with very small differences of 4% at 0.71 Hz shown in Figure 4.2-7b, that are hardly visible and are negligible.

4.2.3 Comparison of Maximum Absolute Accelerations

Tables 4.2-1a and 4.2-1b present the comparisons of the MSM and DM analyses results for the maximum absolute accelerations at all floor and oscillator mass nodes of the FWSC model. The comparisons show that the differences between the DM and MSM analyses results for the maximum accelerations are less than 2%.



4.2.4 Comparison of Maximum Forces and Moments

Tables 4.2-2a and 4.2-2b present the comparisons of the MSM and DM analyses results for the maximum forces and moments for all of the stick elements of the FWSC model. The comparisons show that the differences between the DM and MSM results for maximum element shear forces and bending moments are less than 3% and are negligible. The maximum difference of 5% occurs in the results for torsion of the FWS stick model.

4.2.5 Comparison of Maximum Relative Displacements

Tables 4.2-3a and 4.2-3b present the comparisons of the MSM and DM analyses results for maximum displacements at all lumped mass node locations relative to the free field. The comparison shows negligible differences between the DM and MSM displacements results that are less than 2%.

5. EF3 MSM BENCHMARKING EVALUATION

In order to demonstrate that the effects of granular fill placed above top of the rock at EF3 site are enveloped by ESBWR standard design, a set of SASSI 2010 analyses were performed of the EF3 RB/FB and CB for the full column profiles. These analyses were performed using the MSM method on fully embedded models with interaction nodes defined on the exterior of the excavated volumes and two additional horizontal planes of interaction nodes in the interior of the excavated volumes. To evaluate the SSSI effects at the EF3 site, SSSI analyses were performed of the CB-FWSC combined models that also used the MSM. These SSSI analyses were performed on models that have interaction nodes on the exterior of the excavated volume and one additional horizontal plane of interaction nodes in the interior of the excavated volume.

MSM benchmarking analyses were performed to demonstrate the accuracy of the EF3 site specific SSI and SSSI analyses of fully embedded models. The results of these MSM benchmarking analyses that were performed for the EF3 RB/FB, CB, and FWSC are also used to demonstrate that the MSM is adequate for the NA3 site-specific SSI and SSSI analyses of fully embedded models. A comprehensive study of the NA3 and EF3 subgrade conditions demonstrates the applicability of the results of these EF3 benchmarking analyses for the NA3 site.

5.1 Results of EF3 Benchmarking Analyses

The MSM benchmarking analyses presented in References 2-e, 2-f and 2-g demonstrated the accuracy of the results obtained from the EF3 site-specific SSI and SSSI analyses of RB/FB, CB, and FWSC fully embedded MSM models. The MSM benchmarking analyses of the EF3 RB/FB and CB were performed on quarter models considering responses obtained from the analyses of:

- a) the DM models with all nodes of the excavated volume specified as interaction nodes.



- b) the MSM models with interaction nodes on the exterior of the excavated volume and one additional horizontal plane of interaction nodes in the interior of the excavated volume.
- c) the MSM models with interaction nodes on the exterior of the excavated volume and two additional horizontal planes of interaction nodes in the interior of the excavated volume.

The MSM benchmarking analyses of the EF3 FWSC were performed on half models considering responses obtained from the analyses of:

- a) the DM models with all nodes of the excavated volume specified as interaction nodes.
- b) the MSM model with interaction nodes only on the exterior of the excavated volume.
- c) the MSM models with interaction nodes on the exterior of the excavated volume and one additional horizontal plane of interaction nodes in the interior of the excavated volume.

The accuracy of the MSM solutions were demonstrated based on comparisons of the MSM and the DM analyses results for transfer functions, ISRS, maximum accelerations, maximum member forces, maximum relative displacements, and maximum lateral pressures at key locations. The comparisons show that besides small differences in transfer function results for the responses of the buildings at frequencies higher than 40 Hz, the differences in ISRS, maximum accelerations, maximum member forces, and maximum relative displacements were negligible ($< 2\%$). The differences in the calculated maximum seismic lateral pressures were also small ($< 8\%$), and their effects on the bending moments and shears in the below grade exterior walls were found to be negligible.

5.2 Comparisons of EF3 and NA3 Subgrade Conditions

The NA3 and the EF3 are both rock sites with granular materials overlaying the rock. The RB/FB and CB are socketed in the NA3 and EF3 in-site rock with concrete fill placed to fill the gap between the rock and the exterior walls of the buildings. The RB/FB and CB are all embedded in granular soil material placed above the rock top elevation. The foundations of the NA3 and EF3 FWSC are both supported by blocks of concrete fill that rest on the surface of the rock stratum and are embedded in granular soil.

Figure 5.2-1 presents the shear wave (S-wave) and compression wave (P-wave) velocities of the NA3 and EF3 Best Estimate (BE) full column subgrade profiles, and shows that the rock stratum at NA3 site is considerably closer to the plant grade resulting in a deeper rock embedment of NA3 RB/FB and CB. The figure also shows that the top soil stratum at NA3 site is considerably thinner and stiffer than the engineered fill at EF3 site. The figures also show that the differences between the stiffness of the softer top soil materials and the underlying rock are more pronounced in the EF3 subgrade profiles. Table 5.2-1 presents the thickness, average shear wave velocities, and the shear column frequencies representing the



dynamic properties of the RB/FB and CB embedment at NA3 and EF3 sites. The table shows that the shear column frequencies of NA3 RB/FB embedment are more than three times higher than the shear column frequencies of the EF3 RB/FB embedment. The shear column frequencies of NA3 CB embedment are almost twice those of the EF3 RB/FB embedment.

5.3 Applicability of EF3 MSM Benchmarking Analyses Results for NA3 Site

The geometry and the properties of the EF3 RB/FB, CB, and FWSC structural models used for the EF3 and NA3 site-specific seismic are virtually identical. The only significant difference between the NA3 and EF3 fully embedded SSI models is in the stiffness of the excavated volume. The comprehensive evaluation of the NA3 and EF3 subgrade conditions in Section 5.2 shows that the NA3 excavated volume models have a considerably higher stiffness and less pronounced soil layers stiffness contrasts which make them less sensitive to errors due to the MSM approximation. Therefore, it can be concluded that the NA3 site-specific SSI and SSSI analyses of fully embedded RB/FB and CB models with configurations of interaction nodes, that is consistent with that of the corresponding EF3 models, will not compromise the accuracy of the SASSI 2010 MSM solutions.

For the difference of configuration of the finite element meshes between NA3 and EF3 excavated volume models, NA3 RB/FB and CB models require a refined mesh for the soil layers above the Zone III rock level in order to capture sufficient input motion energy at high frequencies as shown in Figures 3.1-1 and 3.2-1, respectively. These models also require a coarser mesh for the soil layers below the Zone III rock level to keep the total number of interaction nodes below the SASSI2010 limit of 20,000. As such, non-uniform mesh and triangular elements are used in the transitional layers. The accuracy of the non-uniform mesh and triangular elements used for NA3 models are demonstrated by comparing the results with the models using uniform mesh, which are very similar to FE3 models in References 2-a and 2-b, respectively.

6. CONCLUSIONS

The followings are the conclusions from the results of the MSM benchmarking evaluation presented in this report:

- The FWSC MSM models with interaction nodes defined at the bottom and the side surfaces of the excavated volume, the ground surface, and the horizontal planes within the excavated volume (EL -1.60m and EL -5.91m for FWSC SSI and EL -0.68m and -5.87m for FWSC-CB SSSI) are adequate for NA3 site-specific SSI and SSSI analyses.
- The RB/FB fully embedded MSM model with interaction nodes defined at the bottom and the side surfaces of the excavated volume, the ground surface, and the horizontal



plane within the excavated volume (EL 0.08m) is adequate for NA3 site-specific SSI and SSSI analyses of full column profiles.

- The CB fully embedded MSM models with interaction nodes defined at the bottom and the side surfaces of the excavated volume, the ground surface, and the two horizontal planes within the excavated volume (EL 0.69m and -4.645m for CB SSI, EL 0.69m and -5.26m for CB-FWSC SSSI and EL 0.10m and -6.17m for CB-RB/FB SSSI) are adequate for NA3 site-specific SSI and SSSI analyses of full column profiles.



Table 3-1 Boundary Conditions of Half Models for Excavated Volume

Direction of Input Motion	Interaction Nodes	YZ-Plane
X-dir.	Pin Support	Anti-Symmetry
Y, Z-dir.	Pin Support	Symmetry

Pin Support: Translations are fixed



Table 3.1-1 UB Soil Layers Properties of RB/FB Excavated Volume Model

Layer No.	Elevation at Top of Layer (m)	Elevation at Bottom of Layer (m)	Unit Weight, γ (t/m ³)	Shear Wave Velocity, V_s (m/sec)	Poisson's Ratio, ν
1	4.50	3.89	2.00	408	0.400
2	3.89	2.37	2.00	437	0.430
3	2.37	0.84	2.08	634	0.470
4	0.84	-0.68	2.08	862	0.420
5	-0.68	-15.50	2.32	1774	0.400

Table 3.1-2 The Ratio of Layer Thickness to the Shortest Shear Wave Length for RB/FB

Elevation (m)	Thickness, h (m)	Shear Wave Velocity, V_s (m/sec)	Shear Wave Length, L (m)	h / L
4.50	0.61	408	5.83	0.10
3.89				
3.89	0.76	437	6.24	0.12
3.13				
3.13	0.76	437	6.24	0.12
2.37				
2.37	0.77	634	9.06	0.08
1.61				
1.61	0.77	634	9.06	0.08
0.84				
0.84	0.76	862	12.31	0.06
0.08				
0.08	0.76	862	12.31	0.06
-0.68				
-0.68	1.32	1774	25.34	0.05
-2.00				
-2.00	2.50	1774	25.34	0.10
-4.50				
-4.50	1.90	1774	25.34	0.07
-6.40				
-6.40	2.00	1774	25.34	0.08
-8.40				
-8.40	2.00	1774	25.34	0.08
-10.40				
-10.40	1.10	1774	25.34	0.04
-11.50				
-11.50	2.00	1774	25.34	0.08
-13.50				
-13.50	2.00	1774	25.34	0.08
-15.50				

**Table 3.1-3 Location of Interaction Nodes within RB/FB Excavated Volume**

Layer	Elevation at Top of Layer (m)	Elevation at Bottom of Layer (m)	Shear Wave Velocity, V_s (m/sec)	Thickness, h (m)	Traveling Time, h/V_s (sec)	Total Traveling Time, $\Sigma(h/V_s)$ (sec)
1	4.50	3.89	408	0.61	0.00150	0.00875
2	3.89	2.37	437	1.52	0.00348	
3	2.37	0.84	634	1.53	0.00241	
4	0.84	-0.34	862	1.18	0.00136	
4	-0.34	-0.68	862	0.35	0.00040	0.00875
5	-0.68	-15.50	1774	14.82	0.00835	

Note: Optimal location of interaction node plane is EL -0.34 m. The location of the plane is adjusted to EL 0.08 m for the excavated volume model. Total traveling time of the lower part of excavated volume (from EL -15.5m to EL 0.08 m) is 0.00923 sec for the model with interaction node plane at EL 0.08m.

Table 3.1-4 Natural Frequencies of RB/FB Excavated Volume Model

Direction	Natural Frequency (Hz)	
	Upper Part of Excavated Volume	Lower Part of Excavated Volume
X-dir.	66.2 (6 th Mode)	57.3 (1 st Mode)
Y-dir.	66.4 (7 th Mode)	60.4 (3 rd Mode)
Z-dir.	> 70	> 70

Note: The lower values are highlighted in yellow.

**Table 3.2-1 UB Soil Layers Properties of CB Excavated Volume Model**

Layer No.	Elevation at Top of Layer (m)	Elevation at Bottom of Layer (m)	Unit Weight, γ (t/m ³)	Shear Wave Velocity, V_s (m/sec)	Poisson's Ratio, ν
1	4.50	2.98	2.00	394	0.340
2	2.98	-0.07	2.00	506	0.470
3	-0.07	-3.12	2.08	621	0.470
4	-3.12	-6.17	2.32	808	0.440
5	-6.17	-12.26	2.32	1014	0.440
6	-12.26	-15.31	2.32	993	0.440



Table 3.2-2 The Ratio of Layer Thickness to the Shortest Shear Wave Length for CB

(a) CB Standalone Model

Elevation (m)	Thickness, h (m)	Shear Wave Velocity, Vs (m/sec)	Shear Wave Length, L (m)	h / L
4.500	0.76	394	5.63	0.14
3.740				
3.740	0.76	394	5.63	0.14
2.980				
2.980	0.77	506	7.23	0.11
2.215				
2.215	0.77	506	7.23	0.11
1.450				
1.450	0.76	506	7.23	0.11
0.690				
0.690	0.76	506	7.23	0.11
-0.070				
-0.070	0.65	621	8.87	0.07
-0.720				
-0.720	0.65	621	8.87	0.07
-1.370				
-1.370	0.63	621	8.87	0.07
-2.000				
-2.000	0.56	621	8.87	0.06
-2.560				
-2.560	0.56	621	8.87	0.06
-3.120				
-3.120	1.53	808	11.54	0.13
-4.645				
-4.645	1.53	808	11.54	0.13
-6.170				
-6.170	1.23	1014	14.49	0.08
-7.400				
-7.400	1.50	1014	14.49	0.10
-8.900				
-8.900	1.50	1014	14.49	0.10
-10.400				
-10.400	1.86	1014	14.49	0.13
-12.260				
-12.260	1.53	993	14.19	0.11
-13.785				
-13.785	1.53	993	14.19	0.11
-15.310				

**Table 3.2-2 The Ratio of Layer Thickness to the Shortest Shear Wave Length for CB
(Continued)**

(b) CB-FWSC Combined Model

Elevation (m)	Thickness, h (m)	Shear Wave Velocity, Vs (m/sec)	Shear Wave Length, L (m)	h / L
4.500	0.76	394	5.63	0.14
3.740				
3.740	0.76	394	5.63	0.14
2.980				
2.980	0.83	506	7.23	0.11
2.150				
2.150	0.70	506	7.23	0.10
1.450				
1.450	0.76	506	7.23	0.11
0.690				
0.690	0.76	506	7.23	0.11
-0.070				
-0.070	0.65	621	8.87	0.07
-0.720				
-0.720	0.65	621	8.87	0.07
-1.370				
-1.370	0.63	621	8.87	0.07
-2.000				
-2.000	0.56	621	8.87	0.06
-2.560				
-2.560	0.56	621	8.87	0.06
-3.120				
-3.120	2.14	808	11.54	0.19
-5.260				
-5.260	2.14	915	13.07	0.16
-7.400				
-7.400	1.50	1014	14.49	0.10
-8.900				
-8.900	1.50	1014	14.49	0.10
-10.400				
-10.400	1.86	1014	14.49	0.13
-12.260				
-12.260	1.53	993	14.19	0.11
-13.785				
-13.785	1.53	993	14.19	0.11
-15.310				



**Table 3.2-2 The Ratio of Layer Thickness to the Shortest Shear Wave Length for CB
(Continued)**

(c) CB-RB/FB Combined Model

Elevation (m)	Thickness, h (m)	Shear Wave Velocity, Vs (m/sec)	Shear Wave Length, L (m)	h / L
4.500	0.76	394	5.63	0.14
3.740				
3.740	0.76	394	5.63	0.14
2.980				
2.980	0.77	506	7.23	0.11
2.215				
2.215	0.77	506	7.23	0.11
1.450				
1.450	0.76	506	7.23	0.11
0.690				
0.690	0.76	506	7.23	0.11
-0.070				
-0.070	0.65	621	8.87	0.07
-0.720				
-0.720	0.65	621	8.87	0.07
-1.370				
-1.370	0.63	621	8.87	0.07
-2.000				
-2.000	0.56	621	8.87	0.06
-2.560				
-2.560	0.56	621	8.87	0.06
-3.120				
-3.120	1.53	808	11.54	0.13
-4.645				
-4.645	1.53	808	11.54	0.13
-6.170				
-6.170	1.23	1014	14.49	0.08
-7.400				
-7.400	1.50	1014	14.49	0.10
-8.900				
-8.900	1.50	1014	14.49	0.10
-10.400				
-10.400	1.86	1014	14.49	0.13
-12.260				
-12.260	1.53	993	14.19	0.11
-13.785				
-13.785	1.53	993	14.19	0.11
-15.310				



Table 3.2-3 Location of Interaction Nodes within CB Excavated Volume

Layer	Elevation at Top of Layer (m)	Elevation at Bottom of Layer (m)	Shear Wave Velocity, Vs (m/sec)	Thickness, h (m)	Traveling Time, h/Vs (sec)	Total Traveling Time, $\Sigma(h/Vs)$ (sec)
1	4.50	2.98	394	1.52	0.00386	0.00922
2	2.98	0.27	506	2.71	0.00536	
2	0.27	-0.07	506	0.34	0.00067	0.00922
3	-0.07	-3.12	621	3.05	0.00491	
4	-3.12	-6.06	808	2.94	0.00364	
4	-6.06	-6.17	808	0.11	0.00014	0.00922
5	-6.17	-12.26	1014	6.09	0.00601	
6	-12.26	-15.31	993	3.05	0.00307	

Note: Optimal locations of interaction node planes are EL 0.27 m and EL -6.06. The locations of the planes are adjusted as shown in Table 3.2-4 for the excavated volume model. Total traveling times of the parts of excavated volume with adjusted interaction node planes are also shown in Table 3.2-4.

Table 3.2-4 Traveling Times of Shear Wave for CB Excavated Volume

Model	Location of Interaction Node Plane (EL:m)		Traveling Time (sec)		
	Plane 1	Plane 2	Upper Part	Middle Part	Lower Part
CB	0.69	-4.645	0.00839	0.00830	0.01096
CB-FWSC	0.69	-5.26	0.00838	0.00906	0.01020
CB-RB/FB	0.10	-6.17	0.00955	0.00902	0.00916



Table 3.2-5 Natural Frequencies of CB Excavated Volume Model

(a) CB Standalone Model

Direction	Natural Frequency (Hz)		
	Upper Part of Excavated Volume	Middle Part of Excavated Volume	Lower Part of Excavated Volume
X-dir.	62.0 (4 th Mode)	67.9 (19 th Mode)	57.7 (2 nd Mode)
Y-dir.	62.5 (6 th Mode)	67.8 (18 th Mode)	59.4 (3 rd Mode)
Z-dir.	> 70	> 70	> 70

*) The lowest values are highlighted in yellow.

(b) CB-FWSC Combined Model

Direction **)	Natural Frequency (Hz)		
	Upper Part of Excavated Volume	Middle Part of Excavated Volume	Lower Part of Excavated Volume
X-dir.	61.9 (4 th Mode)	63.8 (6 th Mode)	60.6 (2 nd Mode)
Y-dir.	62.3 (2 nd Mode)	63.8 (4 th Mode)	61.6 (1 st Mode)
Z-dir.	> 70	> 70	> 70

*) The lowest values are highlighted in yellow.

**) See Table 3-1 for definition of boundary conditions (BC)

(c) CB-RB/FB Combined Model

Direction	Natural Frequency (Hz)		
	Upper Part of Excavated Volume	Middle Part of Excavated Volume	Lower Part of Excavated Volume
X-dir.	54.1 (3 rd Mode)	63.1 (27 th Mode)	65.4 (33 rd Mode)
Y-dir.	53.9 (2 nd Mode)	63.1 (26 th Mode)	> 70
Z-dir.	> 70	> 70	> 70

*) The lowest values are highlighted in yellow.

**Table 3.3-1 UB Soil Layers Properties of FWSC Excavated Volume Model**

Layer No.	Elevation at Top of Layer (m)	Elevation at Bottom of Layer (m)	Unit Weight, γ (t/m ³)	Shear Wave Velocity, V_s (m/sec)	Poisson Ratio, ν
1	2.15	-1.60	2.00	348	0.470
2	-1.60	-6.78	2.00	483	0.470
3	-6.78	-8.00	2.08	600	0.470
4	-8.00	-9.52	2.08	814	0.440
5	-9.52	-14.40	2.32	1002	0.440
6	-14.40	-16.84	2.32	1028	0.440

**Table 3.3-2 The Ratio of Layer Thickness to the Shortest Shear Wave Length for FWSC**

(a) FWSC Standalone Model

Elevation (m)	Thickness, h (m)	Shear Wave Velocity, Vs (m/sec)	Shear Wave Length, L (m)	h / L
2.150	0.75	348	4.97	0.15
1.400				
1.400	0.75	348	4.97	0.15
0.650				
0.650	0.75	348	4.97	0.15
-0.100				
-0.100	0.75	348	4.97	0.15
-0.850				
-0.850	0.75	348	4.97	0.15
-1.600				
-1.600	0.86	483	6.90	0.12
-2.460				
-2.460	0.86	483	6.90	0.12
-3.320				
-3.320	0.86	483	6.90	0.12
-4.180				
-4.180	0.86	483	6.90	0.12
-5.040				
-5.040	0.87	483	6.90	0.13
-5.910				
-5.910	0.87	483	6.90	0.13
-6.780				
-6.780	1.22	600	8.57	0.14
-8.000				
-8.000	1.52	814	11.63	0.13
-9.520				
-9.520	1.62	1002	14.31	0.11
-11.140				
-11.140	1.63	1002	14.31	0.11
-12.770				
-12.770	1.63	1002	14.31	0.11
-14.400				
-14.400	1.22	1028	14.69	0.08
-15.620				
-15.620	1.22	1028	14.69	0.08
-16.840				



Table 3.3-2 The Ratio of Layer Thickness to the Shortest Shear Wave Length for FWSC (Continued)

(b) FWSC-CB Combined Model

Elevation (m)	Thickness, h (m)	Shear Wave Velocity, Vs (m/sec)	Shear Wave Length, L (m)	h / L
2.150	0.70	348	4.97	0.14
1.450				
1.450	0.70	348	4.97	0.14
0.750				
0.750	0.75	348	4.97	0.15
0.000				
0.000	0.68	348	4.97	0.14
-0.680				
-0.680	0.72	348	4.97	0.14
-1.400				
-1.400	0.60	428	6.11	0.10
-2.000				
-2.000	0.51	483	6.90	0.07
-2.510				
-2.510	0.66	483	6.90	0.10
-3.170				
-3.170	0.90	483	6.90	0.13
-4.070				
-4.070	0.90	483	6.90	0.13
-4.970				
-4.970	0.90	483	6.90	0.13
-5.870				
-5.870	0.91	483	6.90	0.13
-6.780				
-6.780	0.62	600	8.57	0.07
-7.400				
-7.400	0.60	600	8.57	0.07
-8.000				
-8.000	0.70	814	11.63	0.06
-8.700				
-8.700	0.82	814	11.63	0.07
-9.520				
-9.520	0.88	1002	14.31	0.06
-10.400				
-10.400	2.00	1002	14.31	0.14
-12.400				
-12.400	2.00	1002	14.31	0.14
-14.400				
-14.400	2.44	1028	14.69	0.17
-16.840				



Table 3.3-3 Location of Interaction Nodes within FWSC Excavated Volume

Layer	Elevation at Top of Layer (m)	Elevation at Bottom of Layer (m)	Shear Wave Velocity, V_s (m/sec)	Thickness, h (m)	Traveling Time, h/V_s (sec)	Total Traveling Time, $\Sigma(h/V_s)$ (sec)
1	2.15	-1.60	348	3.75	0.01078	0.01088
2	-1.60	-1.65	483	0.05	0.00010	
2	-1.65	-6.78	483	5.13	0.01062	0.01088
3	-6.78	-6.94	600	0.16	0.00026	
3	-6.94	-8.00	600	1.06	0.00177	0.01088
4	-8.00	-9.52	814	1.52	0.00187	
5	-9.52	-14.40	1002	4.88	0.00487	
6	-14.40	-16.84	1028	2.44	0.00237	

Note: Optimal locations of interaction node planes are EL -1.65 m and EL -6.94 m. The locations of the planes are adjusted as shown in Table 3.3-4 for the excavated volume model. Total traveling times of the parts of excavated volume with adjusted interaction node planes are also shown in Table 3.3-4.

Table 3.3-4 Traveling Times of Shear Wave for FWSC Excavated Volume

Model	Location of Interaction Node Plane (EL: m)		Traveling Time (sec)		
	Plane 1	Plane 2	Upper Part	Middle Part	Lower Part
FWSC	-1.60	-5.91	0.01078	0.00892	0.01294
FWSC-CB	-0.68	-5.87	0.00813	0.01109	0.01302

**Table 3.3-5 Natural Frequencies of FWSC Excavated Volume Model****(a) FWSC Standalone Model**

Direction**)	Natural Frequency (Hz)		
	Upper Part of Excavated Volume	Middle Part of Excavated Volume	Lower Part of Excavated Volume
X-dir.	49.3 (2 nd Mode)	60.4 (17 th Mode)	48.5 (1 st Mode)
Y-dir.	50.2 (1 st Mode)	61.7 (17 th Mode)	57.1 (9 th Mode)
Z-dir.	> 70	> 70	> 70

*) The lowest values are highlited in yellow.

**) See Table 3-1 for defintion of boundary conditions (BC)

(b) FWSC-CB Combined Model

Direction**)	Natural Frequency (Hz)		
	Upper Part of Excavated Volume	Middle Part of Excavated Volume	Lower Part of Excavated Volume
X-dir.	64.0 (37 th Mode)	44.2 (2 nd Mode)	42.8 (1 st Mode)
Y-dir.	64.1 (33 rd Mode)	44.5 (1 st Mode)	46.1 (2 nd Mode)
Z-dir.	> 70	> 70	> 70

*) The lowest values are highlited in yellow.

**) See Table 3-1 for defintion of boundary conditions (BC)



Table 4-1 Summary of Excavated Volumes Eigenvalue Analyses Results

Model	Interaction Node Plane	Freq.
RB/FB	7 Planes	57.3 Hz
CB	8 Planes	57.7 Hz
CB-FWSC	8 Planes	60.6 Hz
CB-RB/FB	9 Planes	53.9 Hz
<u>FWSC</u>	7 Planes	48.5 Hz
<u>FWSC-CB</u>	8 Planes	42.8 Hz



Table 4.1-1a Location of Interaction Nodes within FWSC Excavated Volume at Upper Bound Subsurface Profiles

Layer	Elevation at Top of Layer (m)	Elevation at Bottom of Layer (m)	Shear Wave Velocity, Vs (m/sec)	Thickness, h (m)	Traveling Time, h/Vs (sec)	Total Traveling Time, $\Sigma(h/Vs)$ (sec)
1	2.15	-1.60	348	3.75	0.01078	0.01088
2	-1.60	-1.65	483	0.05	0.00010	
2	-1.65	-6.78	483	5.13	0.01062	0.01088
3	-6.78	-6.94	600	0.16	0.00026	
3	-6.94	-8.00	600	1.06	0.00177	0.01088
4	-8.00	-9.52	814	1.52	0.00187	
5	-9.52	-14.40	1002	4.88	0.00487	
6	-14.40	-16.84	1028	2.44	0.00237	

Note: Optimal location of interaction node planes are at EL -1.65 m and EL -6.94 m. The location of the planes are adjusted to EL -1.60 m and EL -5.91 m for the excavated volume model. Total traveling time of the lower part of excavated volume (from EL -16.84 m to EL -5.91 m) is 0.01294 sec for the model with interaction node planes at EL EL -1.60 m and EL -5.91 m.

Table 4.1-1b Location of Interaction Nodes within FWSC Excavated Volume at Lower Bound Subsurface Profiles

Layer	Elevation at Top of Layer (m)	Elevation at Bottom of Layer (m)	Shear Wave Velocity, Vs (m/sec)	Thickness, h (m)	Traveling Time, h/Vs (sec)	Total Traveling Time, $\Sigma(h/Vs)$ (sec)
1	2.15	-1.44	147	3.59	0.02441	0.02441
1	-1.44	-1.60	147	0.16	0.00111	
2	-1.60	-5.89	184	4.29	0.02330	0.02441
2	-5.89	-6.78	184	0.89	0.00485	
3	-6.78	-8.00	310	1.22	0.00394	
4	-8.00	-9.52	436	1.52	0.00349	
5	-9.52	-14.40	581	4.88	0.00840	
6	-14.40	-16.84	655	2.44	0.00373	

Note: Optimal location of interaction node planes are at EL -1.44 m and EL -5.89 m. The location of the planes are adjusted to EL -1.60 m and EL -5.91 m for the excavated volume model. Total traveling time of the lower part of excavated volume (from EL -16.84 m to EL -5.91 m) is 0.02429 sec for the model with interaction node planes at EL EL -1.60 m and EL -5.91 m.



Table 4.2-1a Comparison of FWSC Maximum Absolute Accelerations from UB Subgrade Profile Analyses

(a) DM

Elev. (m)	Node No.	Stick Model	X-dir. (g)	Y-dir. (g)	Z-dir. (g)
19.70	10	FWS	2.2	2.3	1.5
17.25	9	FWS	2.1	2.2	1.5
15.53	8	FWS	1.9	1.9	1.5
13.81	7	FWS	1.7	1.7	1.4
12.10	6	FWS	1.5	1.4	1.3
11.00	5	FWS	1.3	1.3	1.3
9.90	4	FWS	1.2	1.2	1.2
8.81	3	FWS	1.0	1.1	1.1
6.73	2	FWS	0.7	0.8	0.9
4.65	8002	FWSC	0.6	0.7	0.7
2.15	8001	FWSC	0.6	0.6	0.9
19.70	11	Oscillator	--	--	4.2
12.10	60	Oscillator	0.1	0.1	--
8.81	30	Oscillator	1.0	1.1	--

(b) MSM (Reference 2-c)

Elev. (m)	Node No.	Stick Model	X-dir. (g)	Y-dir. (g)	Z-dir. (g)
19.70	10	FWS	2.2	2.3	1.5
17.25	9	FWS	2.1	2.2	1.5
15.53	8	FWS	1.9	1.9	1.5
13.81	7	FWS	1.7	1.7	1.4
12.10	6	FWS	1.5	1.4	1.3
11.00	5	FWS	1.3	1.3	1.3
9.90	4	FWS	1.2	1.2	1.2
8.81	3	FWS	1.0	1.1	1.1
6.73	2	FWS	0.7	0.8	0.9
4.65	8002	FWSC	0.6	0.7	0.7
2.15	8001	FWSC	0.6	0.6	0.9
19.70	11	Oscillator	--	--	4.2
12.10	60	Oscillator	0.1	0.1	--
8.81	30	Oscillator	1.0	1.1	--

(c) Ratio DM/MSM

Elev. (m)	Node No.	Stick Model	X-dir.	Y-dir.	Z-dir.
19.70	10	FWS	100%	100%	100%
17.25	9	FWS	100%	100%	100%
15.53	8	FWS	100%	100%	100%
13.81	7	FWS	100%	100%	100%
12.10	6	FWS	100%	100%	100%
11.00	5	FWS	100%	99%	100%
9.90	4	FWS	100%	99%	100%
8.81	3	FWS	100%	99%	100%
6.73	2	FWS	100%	100%	100%
4.65	8002	FWSC	100%	100%	100%
2.15	8001	FWSC	100%	100%	100%
19.70	11	Oscillator	--	--	100%
12.10	60	Oscillator	100%	100%	--
8.81	30	Oscillator	100%	99%	--

Elev. (m)	Node No.	Stick Model	X-dir. (g)	Y-dir. (g)	Z-dir. (g)
8.25	405	FPE	0.8	1.6	0.7
6.45	402	FPE	0.7	1.1	0.7

Elev. (m)	Node No.	Stick Model	X-dir. (g)	Y-dir. (g)	Z-dir. (g)
8.25	405	FPE	0.8	1.6	0.7
6.45	402	FPE	0.7	1.1	0.7

Elev. (m)	Node No.	Stick Model	X-dir.	Y-dir.	Z-dir.
8.25	405	FPE	100%	100%	100%
6.45	402	FPE	100%	100%	100%



Table 4.2-1b Comparison of FWSC Maximum Absolute Accelerations from LB Subgrade Profile Analyses

(a) DM

Elev. (m)	Node No.	Stick Model	X -dir. (g)	Y-dir. (g)	Z-dir. (g)
19.70	10	FWS	1.5	1.4	0.7
17.25	9	FWS	1.4	1.3	0.7
15.53	8	FWS	1.3	1.2	0.7
13.81	7	FWS	1.1	1.1	0.7
12.10	6	FWS	1.0	1.0	0.7
11.00	5	FWS	0.9	0.9	0.6
9.90	4	FWS	0.9	0.8	0.6
8.81	3	FWS	0.8	0.7	0.6
6.73	2	FWS	0.6	0.6	0.6
4.65	8002	FWSC	0.5	0.5	0.5
2.15	8001	FWSC	0.5	0.5	0.7
19.70	11	Oscillator	--	--	2.1
12.10	60	Oscillator	0.1	0.1	--
8.81	30	Oscillator	0.8	0.7	--

(b) MSM (Reference 2-c)

Elev. (m)	Node No.	Stick Model	X -dir. (g)	Y-dir. (g)	Z-dir. (g)
19.70	10	FWS	1.5	1.4	0.7
17.25	9	FWS	1.4	1.3	0.7
15.53	8	FWS	1.3	1.2	0.7
13.81	7	FWS	1.1	1.1	0.7
12.10	6	FWS	1.0	1.0	0.7
11.00	5	FWS	0.9	0.9	0.6
9.90	4	FWS	0.9	0.8	0.6
8.81	3	FWS	0.8	0.7	0.6
6.73	2	FWS	0.6	0.6	0.6
4.65	8002	FWSC	0.5	0.5	0.5
2.15	8001	FWSC	0.5	0.5	0.7
19.70	11	Oscillator	--	--	2.1
12.10	60	Oscillator	0.1	0.1	--
8.81	30	Oscillator	0.8	0.7	--

(c) Ratio DM/MSM

Elev. (m)	Node No.	Stick Model	X -dir.	Y-dir.	Z-dir.
19.70	10	FWS	100%	100%	100%
17.25	9	FWS	100%	100%	100%
15.53	8	FWS	100%	100%	100%
13.81	7	FWS	100%	100%	100%
12.10	6	FWS	100%	100%	100%
11.00	5	FWS	100%	100%	100%
9.90	4	FWS	100%	100%	100%
8.81	3	FWS	100%	101%	100%
6.73	2	FWS	100%	100%	100%
4.65	8002	FWSC	100%	101%	100%
2.15	8001	FWSC	100%	101%	100%
19.70	11	Oscillator	--	--	100%
12.10	60	Oscillator	100%	100%	--
8.81	30	Oscillator	100%	101%	--

Elev. (m)	Node No.	Stick Model	X -dir. (g)	Y-dir. (g)	Z-dir. (g)
8.25	405	FPE	0.5	0.7	0.5
6.45	402	FPE	0.5	0.6	0.5

Elev. (m)	Node No.	Stick Model	X -dir. (g)	Y-dir. (g)	Z-dir. (g)
8.25	405	FPE	0.6	0.7	0.5
6.45	402	FPE	0.5	0.6	0.5

Elev. (m)	Node No.	Stick Model	X -dir.	Y-dir.	Z-dir.
8.25	405	FPE	99%	100%	100%
6.45	402	FPE	100%	100%	100%

**Table 4.2-2a Comparison of FWSC Maximum Response Forces and Moments from UB Subgrade Profile Analyses****(a) DM**

Elev. (m)	Node No.	Elem No.	Shear		Moment		Torsion (MN-m)
			X-dir. (MN)	Y-dir. (MN)	X-dir. (MN-m)	Y-dir. (MN-m)	
19.70	10	9			5	4	
	9		4.8	5.0	16	15	1.2
17.25	9	8			25	22	
	8		11.7	12.3	45	42	3.7
15.53	8	7			54	49	
	7		16.3	17.1	80	78	6.0
13.81	7	6			89	83	
	6		20.4	21.3	120	120	8.2
12.10	6	5			127	124	
	5		23.4	24.1	149	150	9.8
11.00	5	4			154	153	
	4		25.5	26.1	178	182	10.8
9.90	4	3			182	185	
	3		27.3	27.7	208	215	11.7
8.81	3	2			213	218	
	2		43.9	42.0	303	306	12.8
6.73	2	1			306	309	
4.65	8002		45.3	44.3	400	399	13.7

Elev. (m)	Node No.	Elem No.	Shear		Moment		Torsion (MN-m)
			X-dir. (MN)	Y-dir. (MN)	X-dir. (MN-m)	Y-dir. (MN-m)	
8.25	402,	405			2	6	
4.65	401	404	4.1	7.5	14	28	5.9

(b) MSM (Reference 2-c)

Elev. (m)	Node No.	Elem No.	Shear		Moment		Torsion (MN-m)
			X-dir. (MN)	Y-dir. (MN)	X-dir. (MN-m)	Y-dir. (MN-m)	
19.70	10	9			5	4	
	9		4.8	5.0	16	15	1.2
17.25	9	8			25	23	
	8		11.7	12.3	45	42	3.6
15.53	8	7			54	49	
	7		16.3	17.1	80	78	5.9
13.81	7	6			88	83	
	6		20.4	21.3	120	120	8.0
12.10	6	5			127	124	
	5		23.4	24.1	149	150	9.5
11.00	5	4			154	153	
	4		25.5	26.1	178	182	10.6
9.90	4	3			182	185	
	3		27.3	27.7	208	214	11.5
8.81	3	2			212	218	
	2		43.9	42.2	303	306	12.5
6.73	2	1			306	309	
4.65	8002		45.3	44.6	400	400	13.4

Elev. (m)	Node No.	Elem No.	Shear		Moment		Torsion (MN-m)
			X-dir. (MN)	Y-dir. (MN)	X-dir. (MN-m)	Y-dir. (MN-m)	
8.25	402,	405			2	6	
4.65	401	404	4.1	7.5	14	28	5.9

(c) Ratio DM/MSM

Elev. (m)	Node No.	Elem No.	Shear		Moment		Torsion
			X-dir.	Y-dir.	X-dir.	Y-dir.	
19.70	10	9			100%	99%	
	9		100%	100%	100%	100%	103%
17.25	9	8			100%	99%	
	8		100%	100%	100%	100%	103%
15.53	8	7			100%	99%	
	7		100%	100%	100%	100%	102%
13.81	7	6			100%	100%	
	6		100%	100%	100%	100%	103%
12.10	6	5			100%	100%	
	5		100%	100%	100%	100%	103%
11.00	5	4			100%	100%	
	4		100%	100%	100%	100%	103%
9.90	4	3			100%	100%	
	3		100%	100%	100%	100%	102%
8.81	3	2			100%	100%	
	2		100%	99%	100%	100%	102%
6.73	2	1			100%	100%	
4.65	8002		100%	99%	100%	100%	102%

Elev. (m)	Node No.	Elem No.	Shear		Moment		Torsion
			X-dir.	Y-dir.	X-dir.	Y-dir.	
8.25	402,	405			100%	101%	
4.65	401	404	100%	100%	100%	100%	100%

**Table 4.2-2b Comparison of FWSC Maximum Response Forces and Moments from LB Subgrade Profile Analyses****(a) DM**

Elev. (m)	Node No.	Elem No.	Shear		Moment		Torsion (MN-m)
			X-dir. (MN)	Y-dir. (MN)	X-dir. (MN-m)	Y-dir. (MN-m)	
19.70	10	9			2	2	
	9		3.2	3.0	9	10	1.4
17.25	9	8			13	14	
	8		7.8	7.5	26	27	4.1
15.53	8	7			30	31	
	7		10.9	10.5	49	49	6.9
13.81	7	6			52	53	
	6		13.7	13.2	76	74	9.5
12.10	6	5			79	78	
	5		15.8	15.1	96	93	11.4
11.00	5	4			98	96	
	4		17.3	16.6	117	112	12.9
9.90	4	3			119	115	
	3		18.6	17.9	139	133	14.2
8.81	3	2			142	136	
	2		31.1	30.1	206	199	16.0
6.73	2	1			209	202	
4.65	8002		32.9	31.8	277	267	17.9

Elev. (m)	Node No.	Elem No.	Shear		Moment		Torsion (MN-m)
			X-dir. (MN)	Y-dir. (MN)	X-dir. (MN-m)	Y-dir. (MN-m)	
8.25	402,	405			1	4	
4.65	401	404	2.8	3.5	9	13	3.7

(b) MSM (Reference 2-c)

Elev. (m)	Node No.	Elem No.	Shear		Moment		Torsion (MN-m)
			X-dir. (MN)	Y-dir. (MN)	X-dir. (MN-m)	Y-dir. (MN-m)	
19.70	10	9			2	2	
	9		3.2	3.0	9	9	1.3
17.25	9	8			13	14	
	8		7.8	7.5	26	26	4.1
15.53	8	7			30	31	
	7		10.9	10.4	49	48	6.7
13.81	7	6			52	52	
	6		13.7	13.1	76	73	9.2
12.10	6	5			78	76	
	5		15.7	15.1	96	92	11.0
11.00	5	4			98	94	
	4		17.2	16.5	116	112	12.4
9.90	4	3			118	114	
	3		18.5	17.8	139	133	13.6
8.81	3	2			141	136	
	2		31.1	30.0	206	198	15.2
6.73	2	1			208	201	
4.65	8002		32.8	31.6	276	267	17.0

Elev. (m)	Node No.	Elem No.	Shear		Moment		Torsion (MN-m)
			X-dir. (MN)	Y-dir. (MN)	X-dir. (MN-m)	Y-dir. (MN-m)	
8.25	402,	405			1	4	
4.65	401	404	2.8	3.5	9	13	3.7

(c) Ratio DM/MSM

Elev. (m)	Node No.	Elem No.	Shear		Moment		Torsion
			X-dir.	Y-dir.	X-dir.	Y-dir.	
19.70	10	9			101%	102%	
	9		100%	100%	100%	102%	102%
17.25	9	8			100%	102%	
	8		100%	100%	100%	102%	102%
15.53	8	7			100%	102%	
	7		100%	100%	100%	102%	102%
13.81	7	6			100%	102%	
	6		100%	100%	100%	102%	103%
12.10	6	5			100%	102%	
	5		100%	100%	100%	102%	104%
11.00	5	4			100%	102%	
	4		100%	100%	100%	101%	104%
9.90	4	3			100%	101%	
	3		100%	100%	100%	100%	105%
8.81	3	2			100%	100%	
	2		100%	100%	100%	100%	105%
6.73	2	1			100%	100%	
4.65	8002		100%	100%	100%	100%	105%

Elev. (m)	Node No.	Elem No.	Shear		Moment		Torsion
			X-dir.	Y-dir.	X-dir.	Y-dir.	
8.25	402,	405			100%	100%	
4.65	401	404	100%	100%	100%	100%	100%



Table 4.2-3a Comparison of FWSC Maximum Relative Displacement from UB Subgrade Profile Analyses

(a) DM

Elev. (m)	Node No.	Stick Model	X -dir. (cm)	Y-dir. (cm)	Z-dir. (cm)
19.70	10	FWS	0.22	0.32	0.03
17.25	9	FWS	0.20	0.31	0.08
15.53	8	FWS	0.19	0.29	0.08
13.81	7	FWS	0.17	0.26	0.08
12.10	6	FWS	0.15	0.24	0.08
11.00	5	FWS	0.14	0.22	0.07
9.90	4	FWS	0.13	0.21	0.07
8.81	3	FWS	0.12	0.19	0.07
6.73	2	FWS	0.09	0.15	0.06
4.65	8002	FWSC	0.07	0.11	0.05
2.15	8001	FWSC	0.07	0.10	0.06

(b) MSM (Reference 2-c)

Elev. (m)	Node No.	Stick Model	X -dir. (cm)	Y-dir. (cm)	Z-dir. (cm)
19.70	10	FWS	0.22	0.33	0.03
17.25	9	FWS	0.20	0.31	0.08
15.53	8	FWS	0.19	0.29	0.08
13.81	7	FWS	0.17	0.26	0.08
12.10	6	FWS	0.15	0.24	0.08
11.00	5	FWS	0.14	0.22	0.07
9.90	4	FWS	0.13	0.21	0.07
8.81	3	FWS	0.12	0.19	0.07
6.73	2	FWS	0.09	0.15	0.06
4.65	8002	FWSC	0.07	0.11	0.05
2.15	8001	FWSC	0.07	0.10	0.06

(c) Ratio DM/MSM

Elev. (m)	Node No.	Stick Model	X -dir.	Y-dir.	Z-dir.
19.70	10	FWS	100%	99%	100%
17.25	9	FWS	100%	99%	100%
15.53	8	FWS	100%	99%	99%
13.81	7	FWS	100%	99%	99%
12.10	6	FWS	100%	99%	99%
11.00	5	FWS	100%	99%	99%
9.90	4	FWS	100%	99%	99%
8.81	3	FWS	100%	99%	99%
6.73	2	FWS	100%	100%	99%
4.65	8002	FWSC	100%	100%	100%
2.15	8001	FWSC	100%	100%	100%

Elev. (m)	Node No.	Stick Model	X -dir. (cm)	Y-dir. (cm)	Z-dir. (cm)
8.25	405	FPE	0.07	0.13	0.03
6.45	402	FPE	0.07	0.12	0.02

Elev. (m)	Node No.	Stick Model	X -dir. (cm)	Y-dir. (cm)	Z-dir. (cm)
8.25	405	FPE	0.07	0.13	0.03
6.45	402	FPE	0.07	0.12	0.02

Elev. (m)	Node No.	Stick Model	X -dir.	Y-dir.	Z-dir.
8.25	405	FPE	100%	100%	99%
6.45	402	FPE	100%	100%	100%



Table 4.2-3b Comparison of FWSC Maximum Relative Displacement from LB Subgrade Profile Analyses

(a) DM

Elev. (m)	Node No.	Stick Model	X -dir. (cm)	Y-dir. (cm)	Z-dir. (cm)
19.70	10	FWS	0.28	0.39	0.05
17.25	9	FWS	0.27	0.36	0.10
15.53	8	FWS	0.25	0.34	0.10
13.81	7	FWS	0.24	0.32	0.10
12.10	6	FWS	0.22	0.30	0.10
11.00	5	FWS	0.21	0.29	0.10
9.90	4	FWS	0.20	0.27	0.09
8.81	3	FWS	0.18	0.26	0.09
6.73	2	FWS	0.15	0.22	0.09
4.65	8002	FWSC	0.12	0.19	0.08
2.15	8001	FWSC	0.12	0.17	0.10

(b) MSM (Reference 2-c)

Elev. (m)	Node No.	Stick Model	X -dir. (cm)	Y-dir. (cm)	Z-dir. (cm)
19.70	10	FWS	0.28	0.39	0.05
17.25	9	FWS	0.27	0.36	0.10
15.53	8	FWS	0.25	0.34	0.10
13.81	7	FWS	0.24	0.32	0.10
12.10	6	FWS	0.22	0.30	0.10
11.00	5	FWS	0.21	0.29	0.10
9.90	4	FWS	0.20	0.27	0.09
8.81	3	FWS	0.18	0.26	0.09
6.73	2	FWS	0.15	0.22	0.09
4.65	8002	FWSC	0.12	0.19	0.08
2.15	8001	FWSC	0.12	0.17	0.10

(c) Ratio DM/MSM

Elev. (m)	Node No.	Stick Model	X -dir.	Y-dir.	Z-dir.
19.70	10	FWS	100%	100%	100%
17.25	9	FWS	100%	100%	100%
15.53	8	FWS	100%	100%	100%
13.81	7	FWS	100%	100%	100%
12.10	6	FWS	100%	100%	100%
11.00	5	FWS	100%	100%	100%
9.90	4	FWS	100%	100%	100%
8.81	3	FWS	100%	100%	100%
6.73	2	FWS	100%	100%	100%
4.65	8002	FWSC	100%	100%	100%
2.15	8001	FWSC	100%	100%	100%

Elev. (m)	Node No.	Stick Model	X -dir. (cm)	Y-dir. (cm)	Z-dir. (cm)
8.25	405	FPE	0.12	0.22	0.06
6.45	402	FPE	0.11	0.20	0.03

Elev. (m)	Node No.	Stick Model	X -dir. (cm)	Y-dir. (cm)	Z-dir. (cm)
8.25	405	FPE	0.12	0.22	0.06
6.45	402	FPE	0.11	0.20	0.03

Elev. (m)	Node No.	Stick Model	X -dir.	Y-dir.	Z-dir.
8.25	405	FPE	100%	100%	99%
6.45	402	FPE	100%	100%	100%



Table 5.2-1 Properties of RB/FB and CB Embedment at NA3 and EF3 Sites

Build.	Site	Soil Case	Rock Embedment			Full Embedment		
			Depth	$V_{s\text{ ave}}$	f_{sc}	Depth	$V_{s\text{ ave}}$	f_{sc}
			m	m/s	Hz	m	m/s	Hz
RB/FB	NA3	LB	14.9	979	16.4	20.1	529	6.6
		BE		1318	22.1		780	9.7
		UB		1774	29.7		1143	14.2
	EF3	LB	9.2	1655	45.1		178	2.2
		BE		2027	55.2		279	3.5
		UB		2483	67.6		433	5.4
CB	NA3	LB	7.3	519	17.8	14.9	304	5.1
		BE		690	23.7		448	7.5
		UB		916	31.5		655	11.0
	EF3	LB	3.5	1620	115.7		158	2.7
		BE		1984	141.7		250	4.2
		UB		2430	173.6		395	6.6

$V_{s\text{ ave}}$: Shear wave velocity

f_{sc} : Shear column frequency

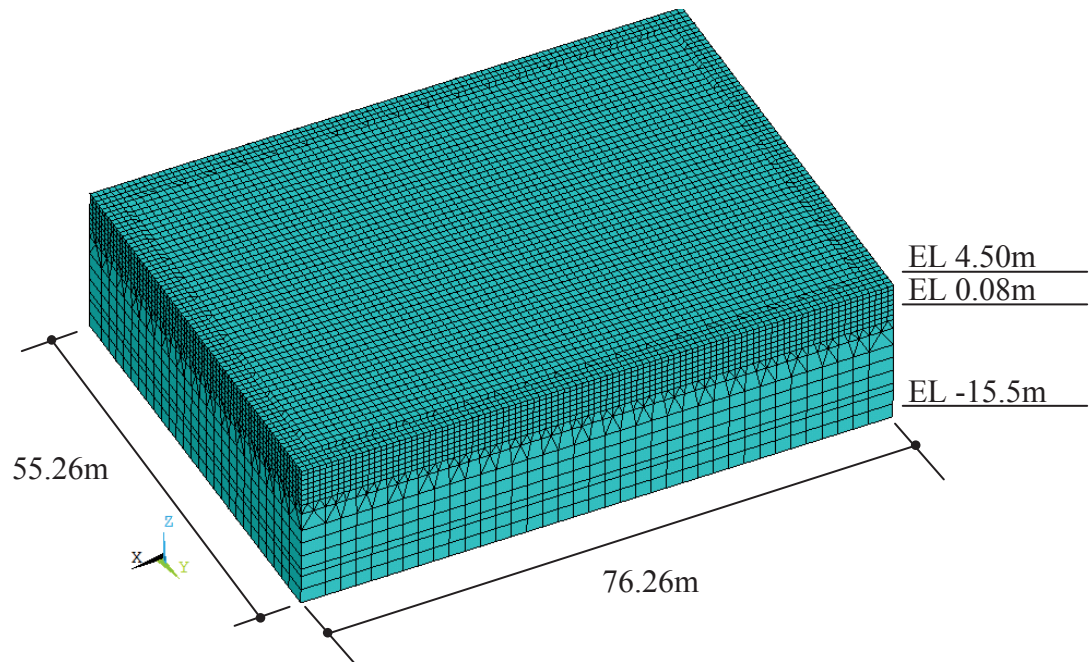
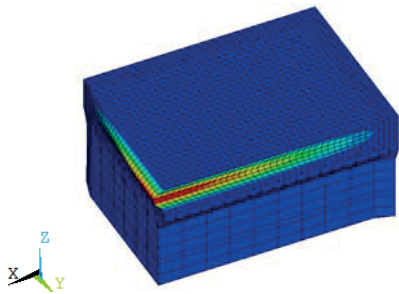
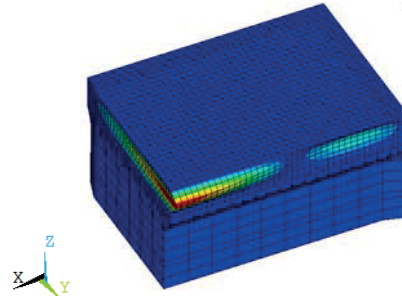


Figure 3.1-1 Soil Layers of RB/FB Excavated Volume Model

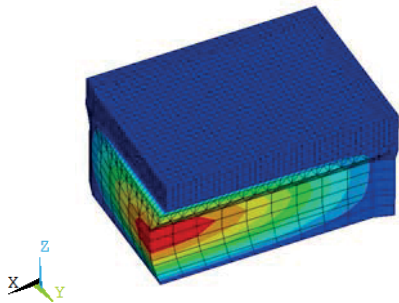


X-dir.

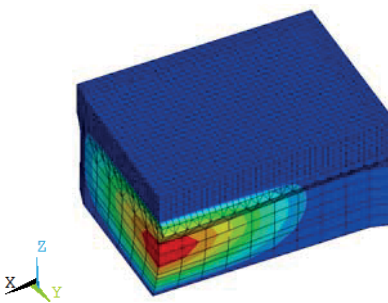


Y-dir.

(a) Upper Part of Excavated Volume



X-dir.



Y-dir.

(b) Lower Part of Excavated Volume

Figure 3.1-2 RB/FB Excavated Volume Mode Shapes

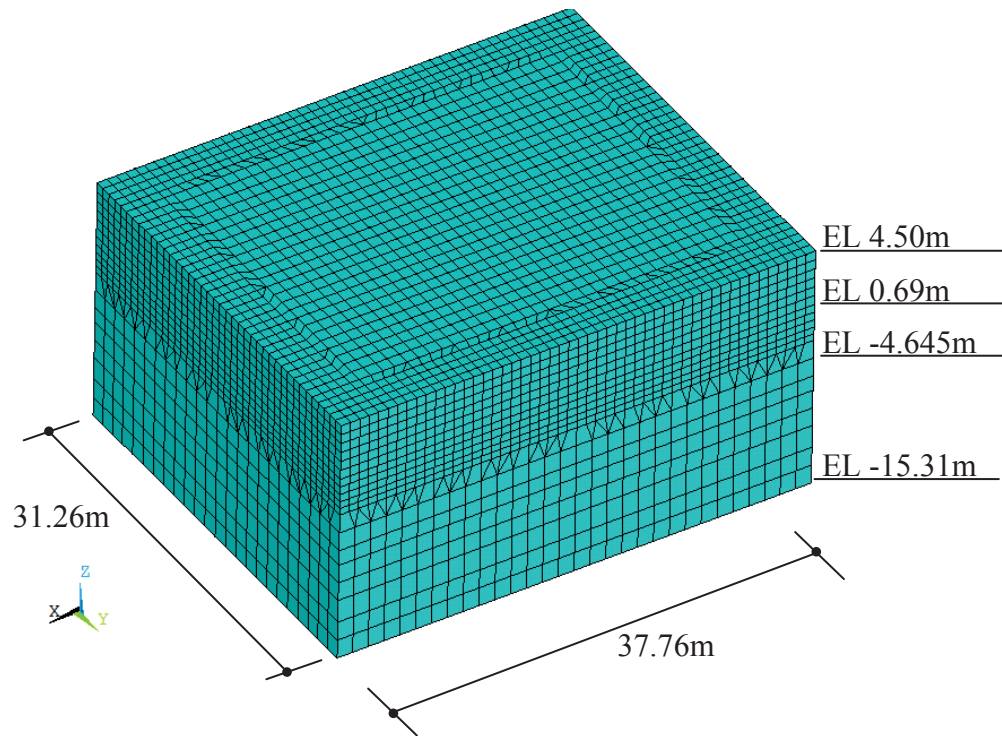


Figure 3.2-1 Soil Layers of CB Standalone Excavated Volume Model

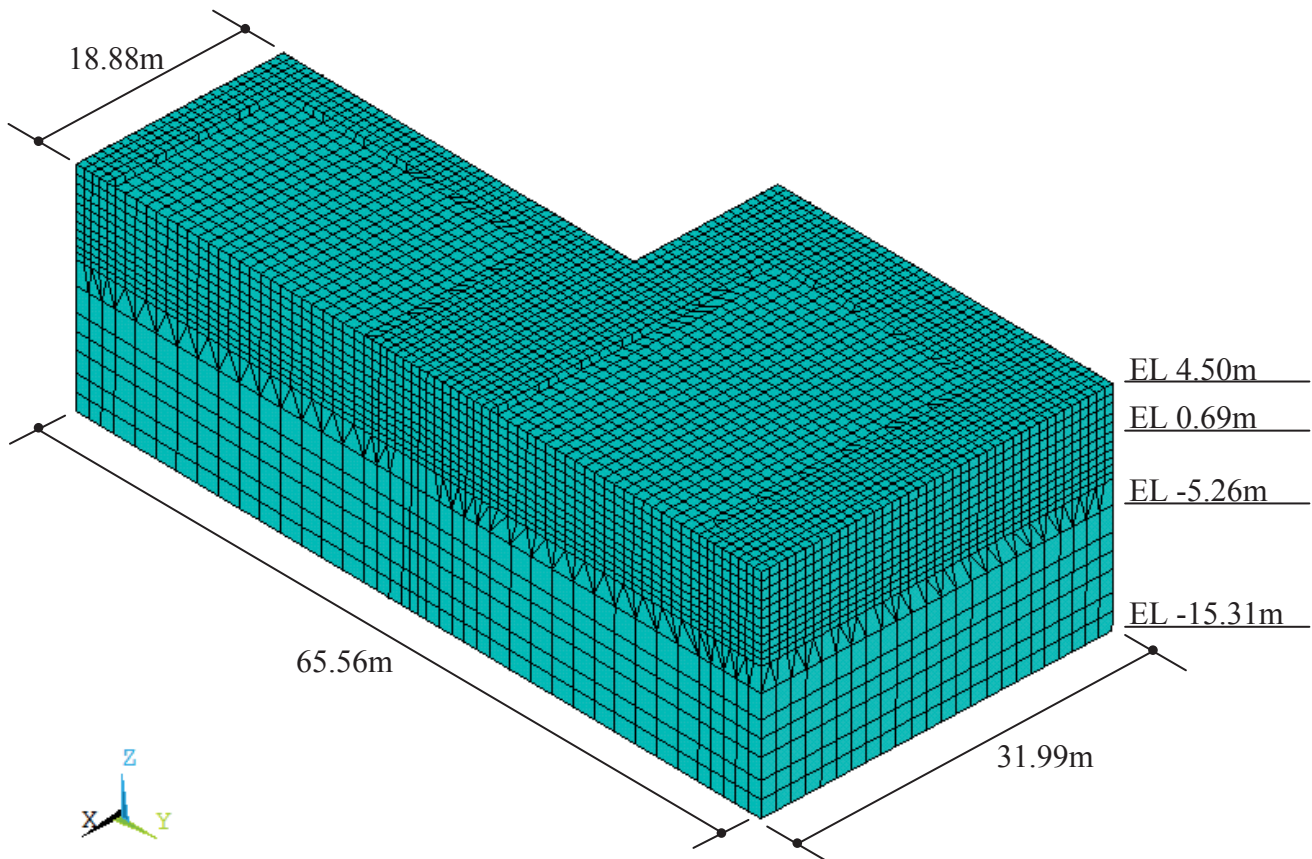


Figure 3.2-2 Soil Layers of CB-FWSC Combined Excavated Volume Half Model

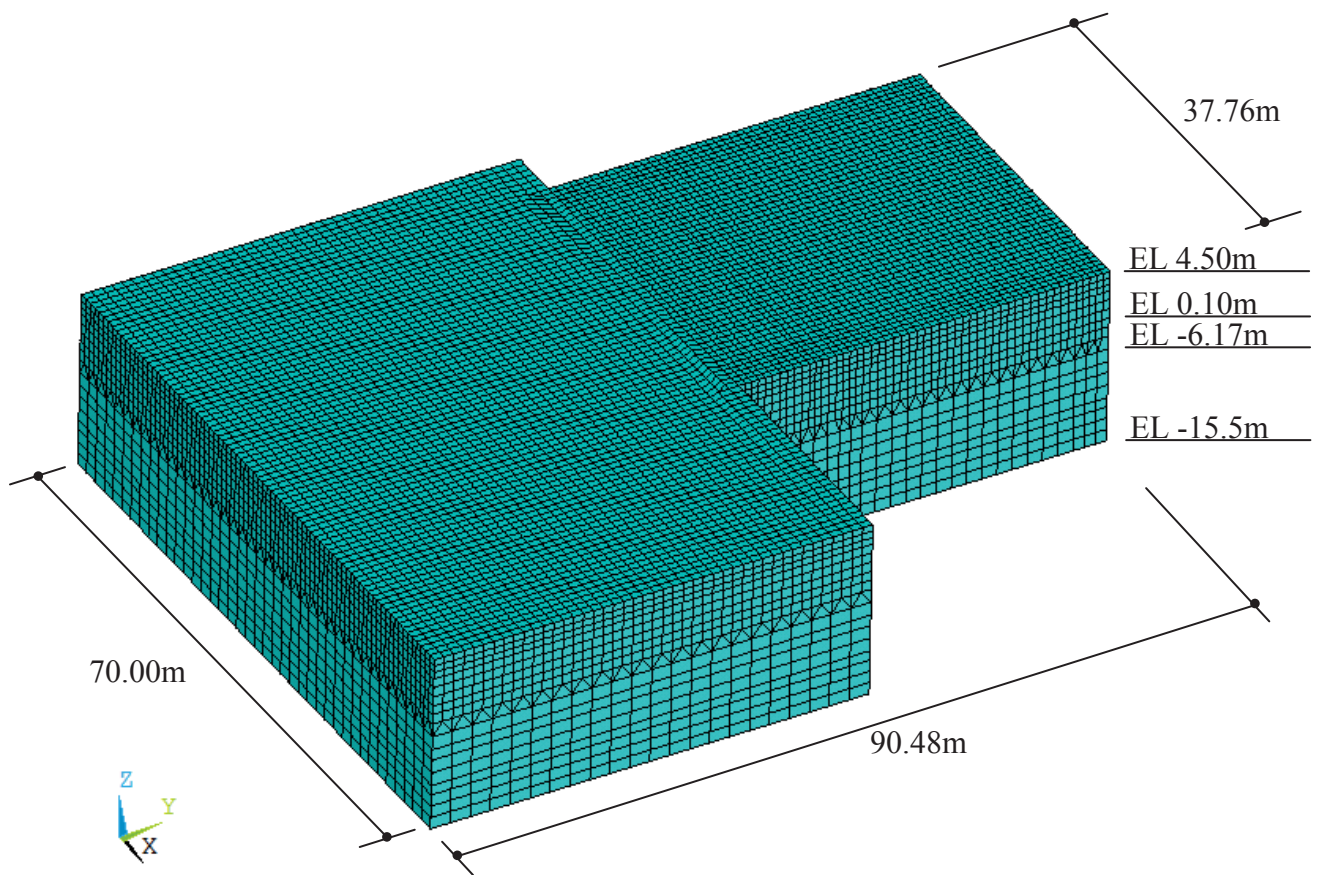
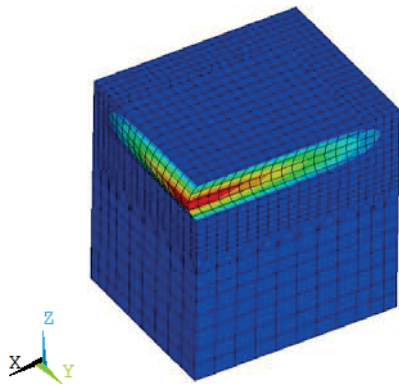
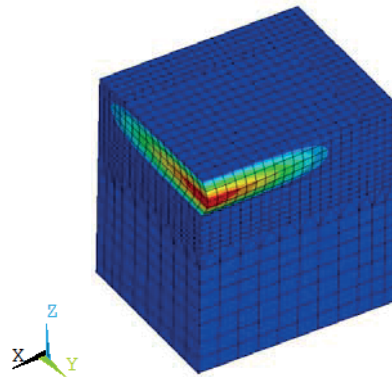


Figure 3.2-3 Soil Layers of CB-RB/FB Combined Excavated Volume Model

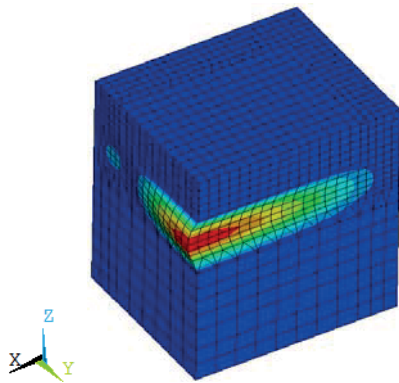


X-dir.

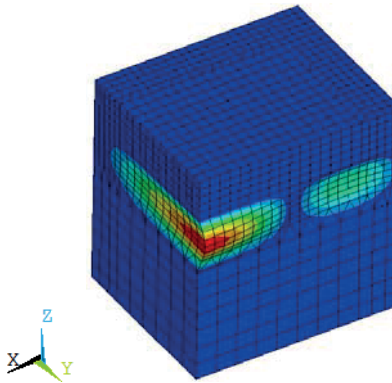


Y-dir.

(a) Upper Part of Excavated Volume

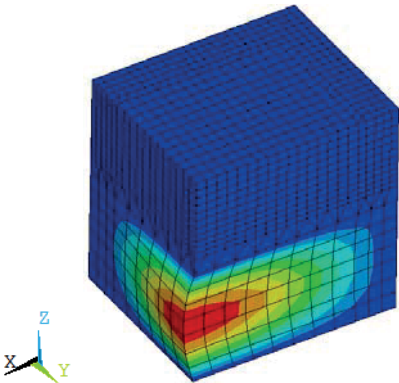


X-dir.

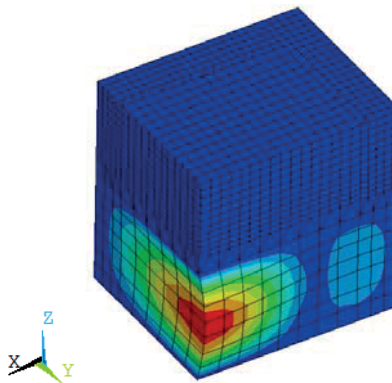


Y-dir.

(b) Middle Part of Excavated Volume



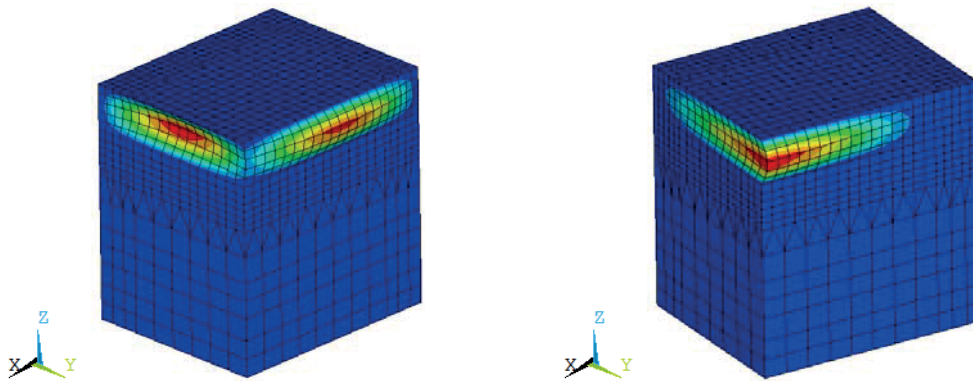
X-dir.



Y-dir.

(c) Lower Part of Excavated Volume

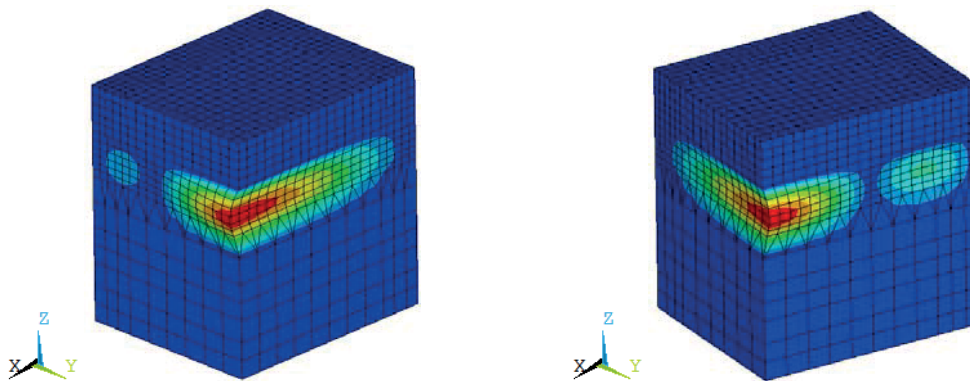
Figure 3.2-4 CB Standalone Excavated Volume Mode Shapes



X-dir.

Y-dir.

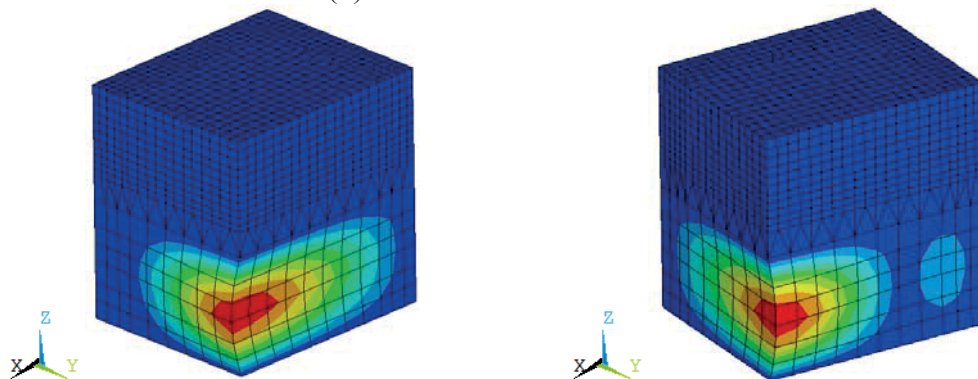
(a) Upper Part of Excavated Volume



X-dir.

Y-dir.

(b) Middle Part of Excavated Volume

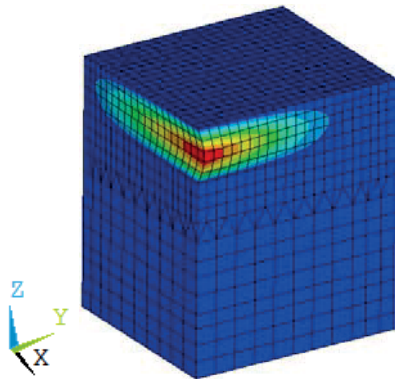


X-dir.

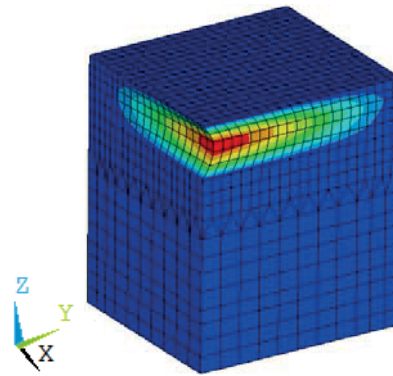
Y-dir.

(c) Lower Part of Excavated Volume

Figure 3.2-5 CB Excavated Volume Mode Shapes for CB-FWSC Combined Model

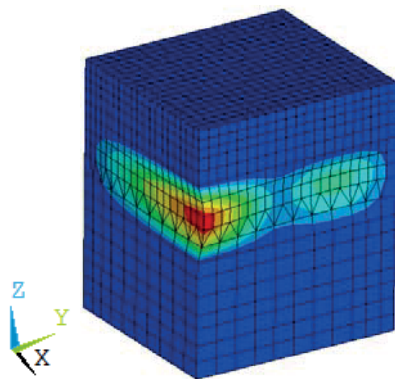


X-dir.

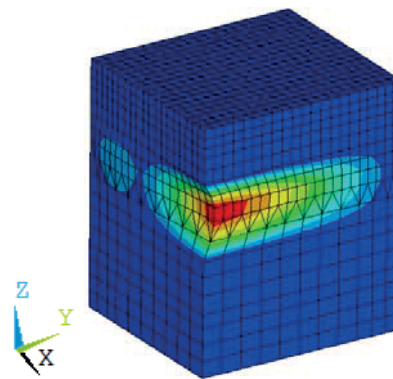


Y-dir.

(a) Upper Part of Excavated Volume

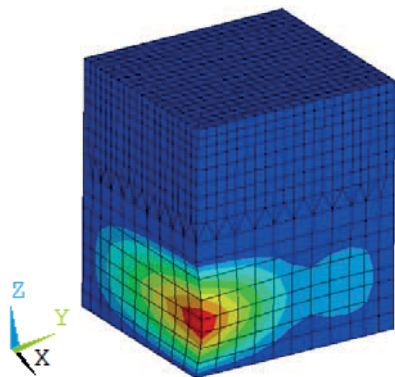


X-dir.



Y-dir.

(b) Middle Part of Excavated Volume



X-dir.

Over
70 Hz

Y-dir.

(c) Lower Part of Excavated Volume

Figure 3.2-6 CB Excavated Volume Mode Shapes for CB-RB/FB Combined Model

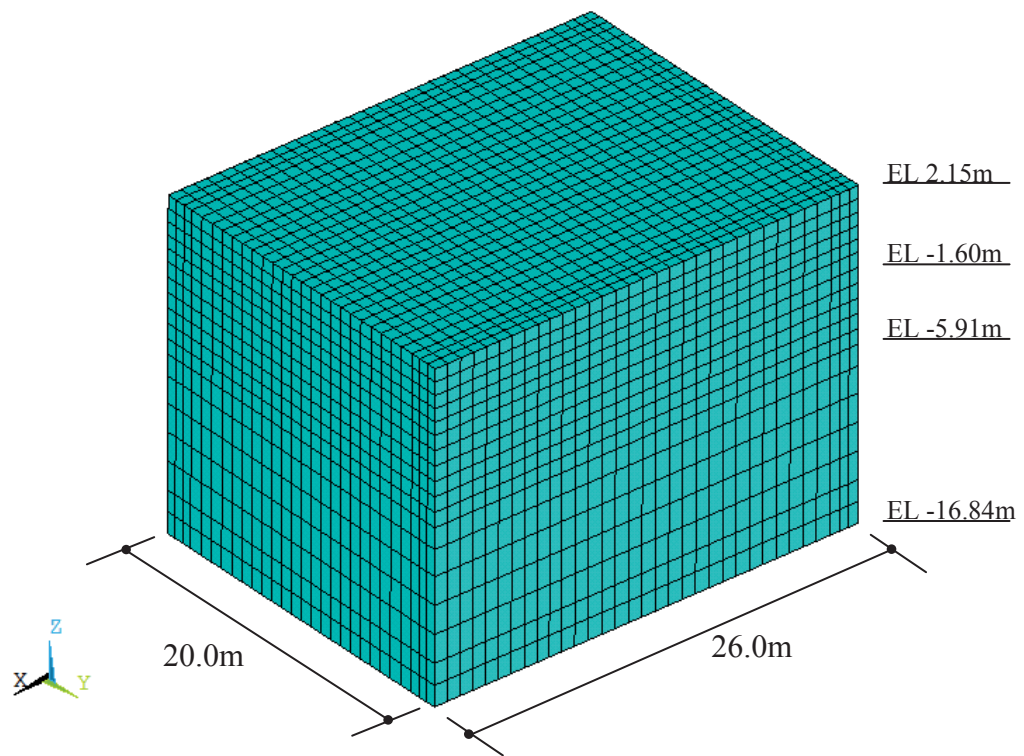


Figure 3.3-1 Soil Layers of FWSC Standalone Excavated Volume Half Model



HITACHI

SER-DMN-011 SH NO. 49
REV. 1 of 74

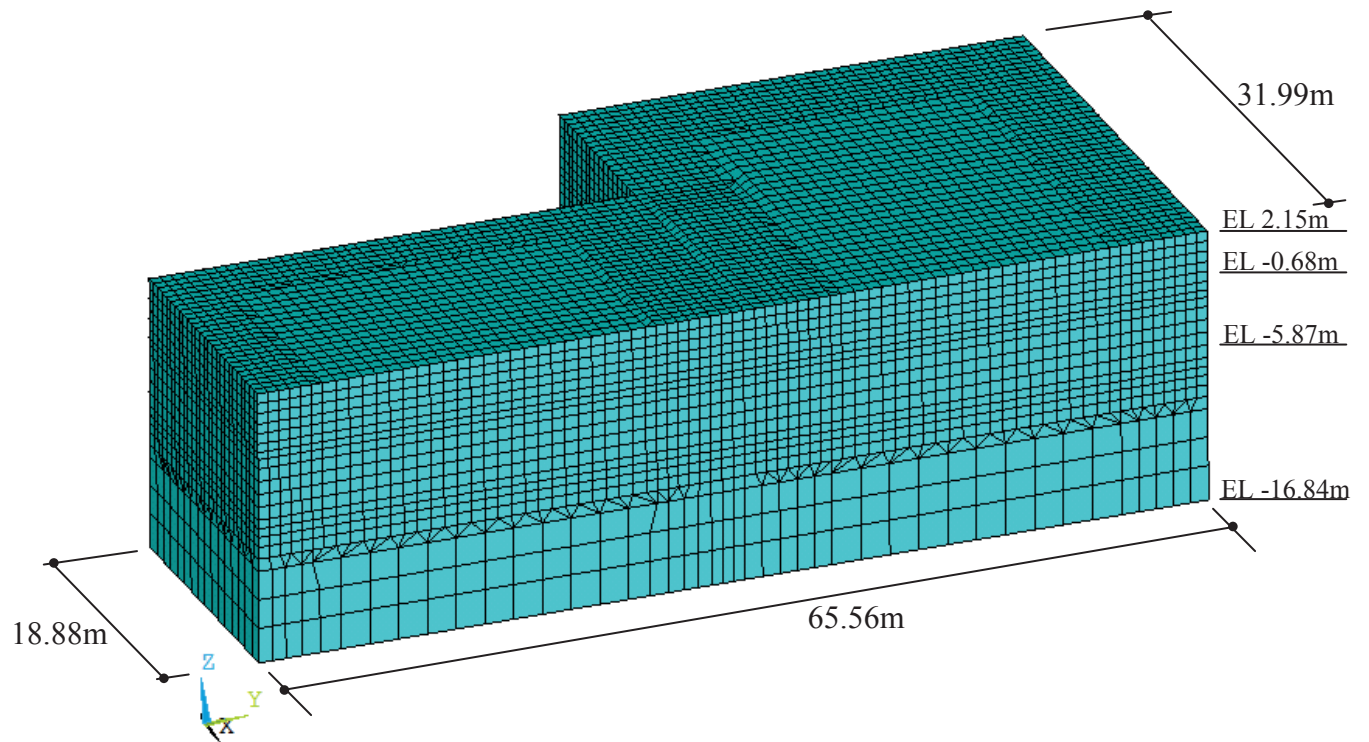
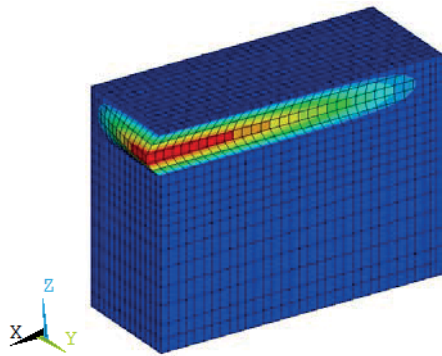
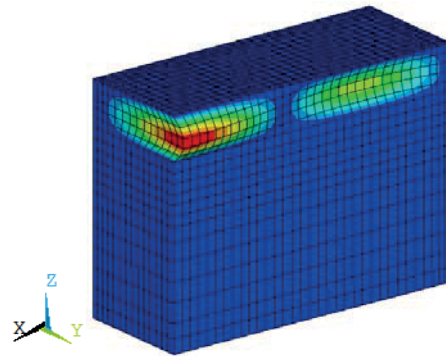


Figure 3.3-2 Soil Layers of FWSC-CB Combined Excavated Volume Half Model

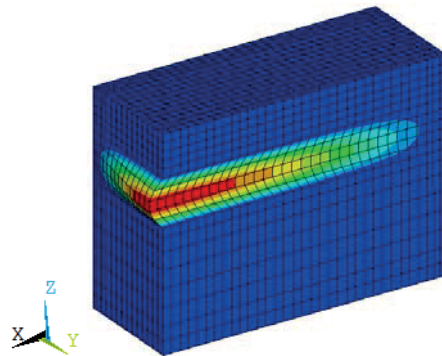


X-dir.

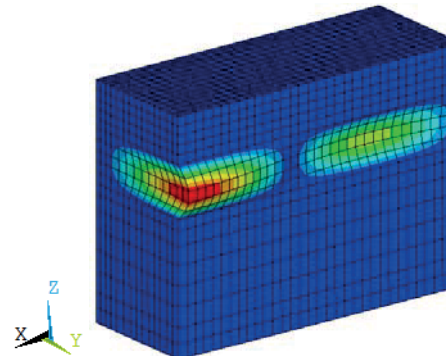


Y-dir.

(a) Upper Part of Excavated Volume

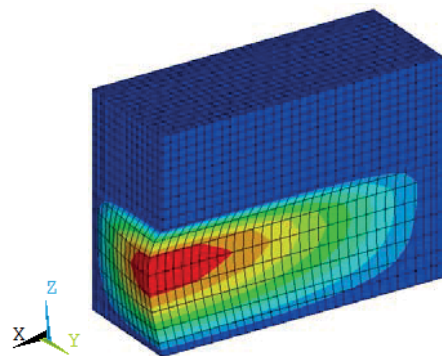


X-dir.

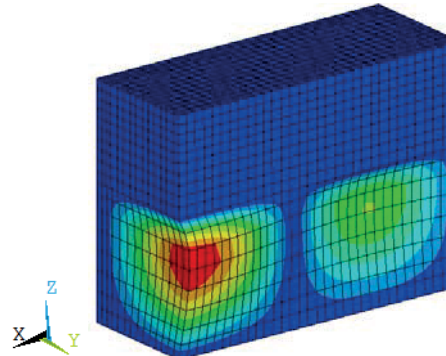


Y-dir.

(b) Middle Part of Excavated Volume



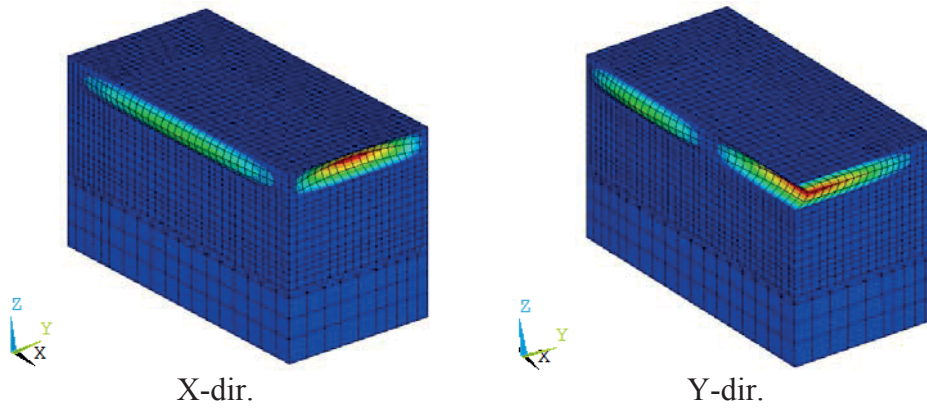
X-dir.



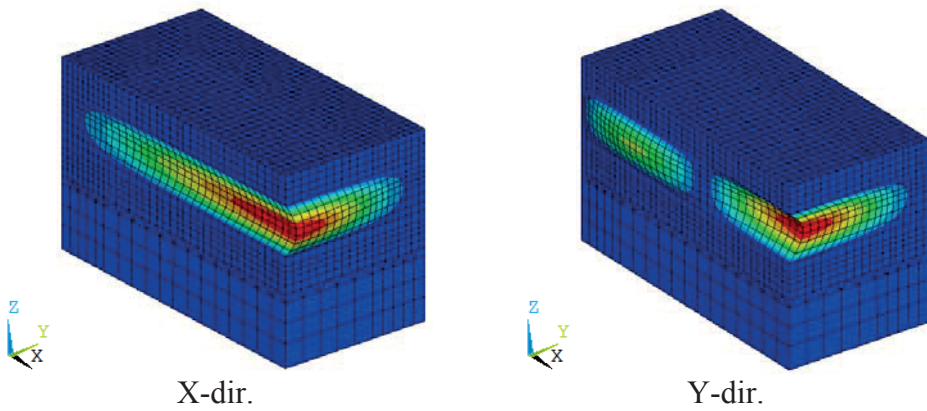
Y-dir.

(c) Lower Part of Excavated Volume

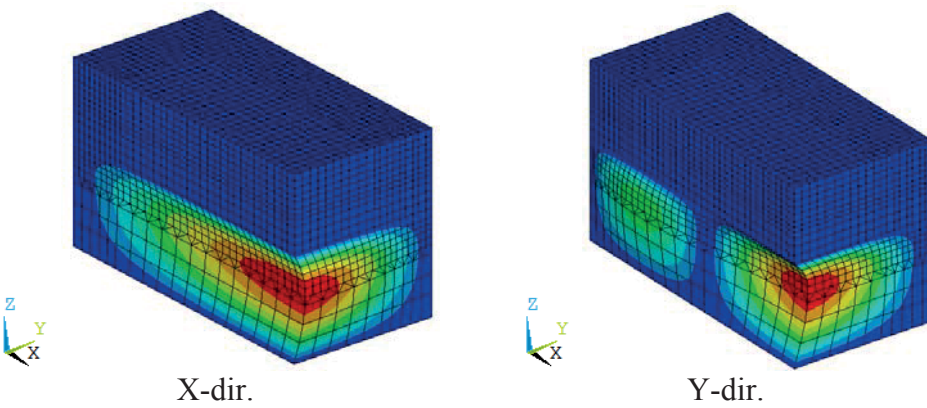
Figure 3.3-3 FWSC Standalone Excavated Volume Mode Shapes



(a) Upper Part of Excavated Volume



(b) Middle Part of Excavated Volume



(c) Lower Part of Excavated Volume

Figure 3.3-4 FWSC Excavated Volume Mode Shapes for FWSC-CB Combined Model



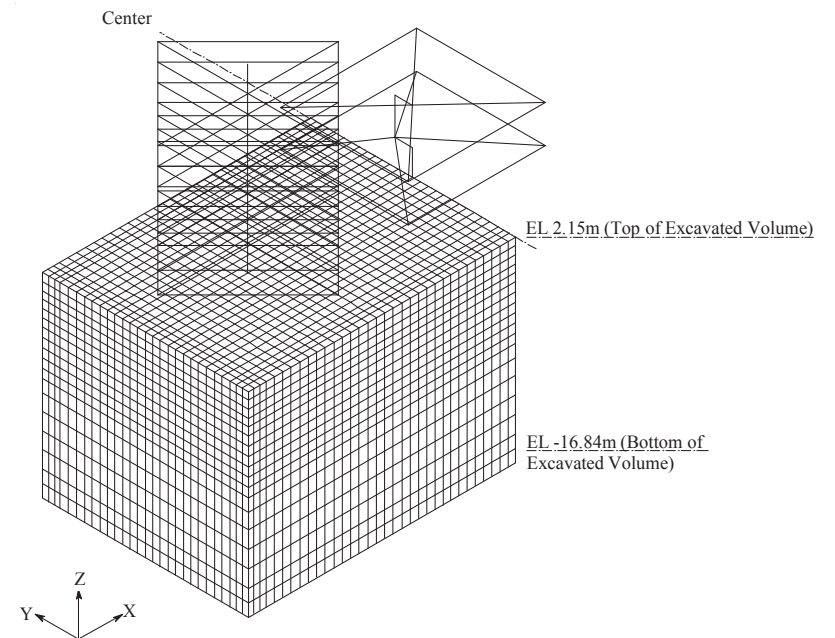
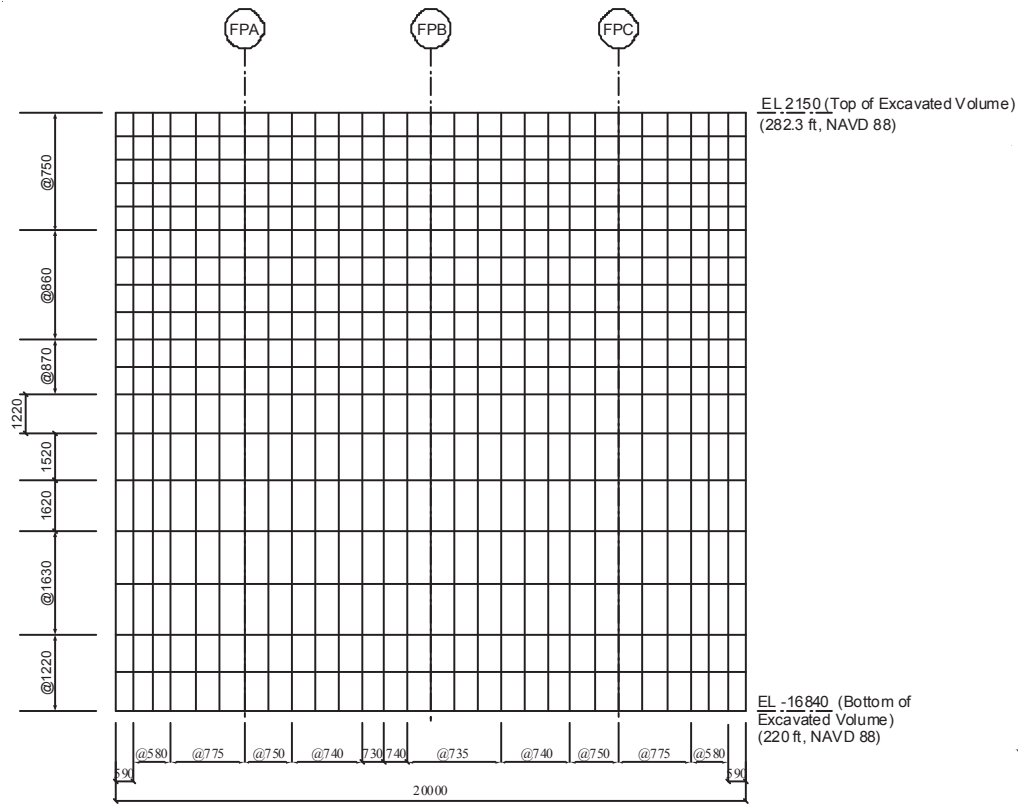
HITACHI

SER-DMN-011

SH NO. 52

REV. 1

of 74



All nodes in excavated volume specified as interaction nodes

Figure 4.1-1 DM Analysis Model for FWSC

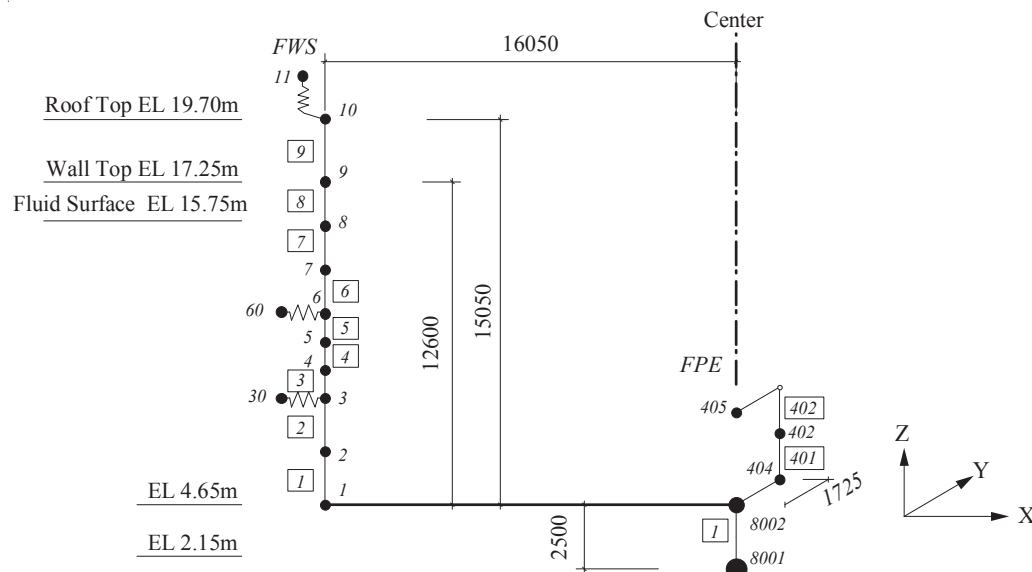
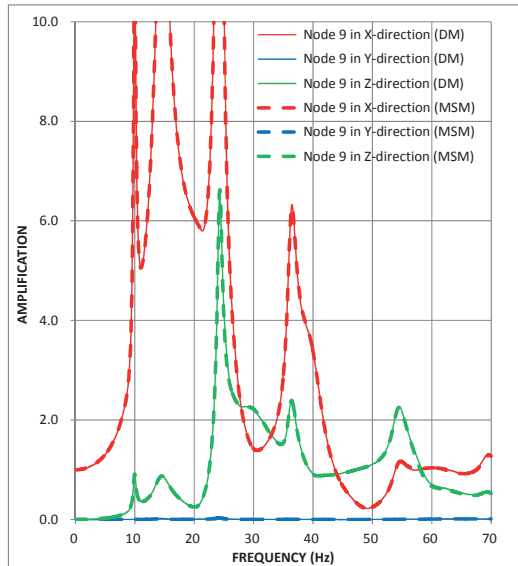
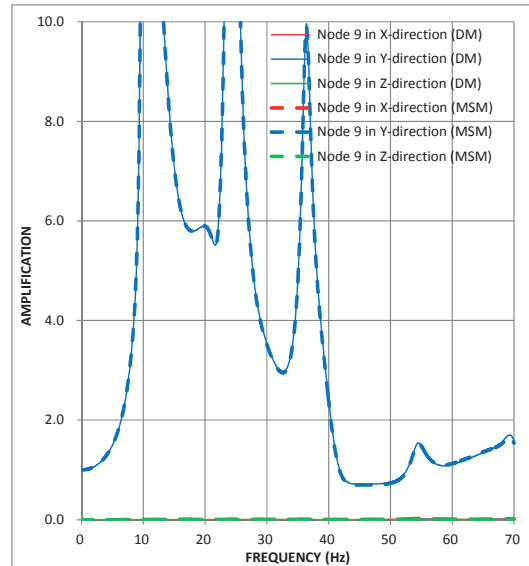


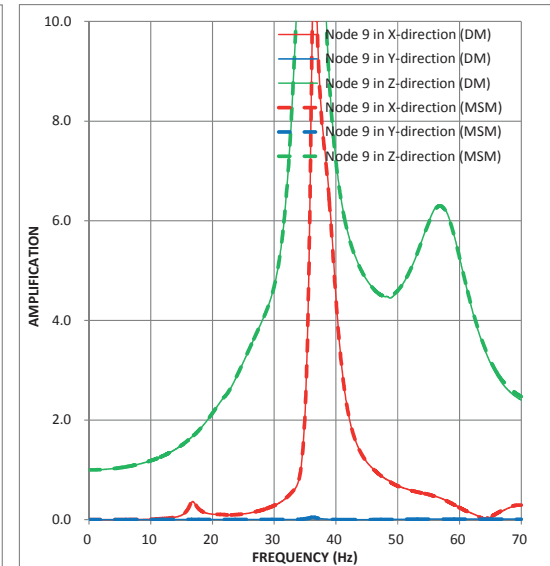
Figure 4.1-2 FWSC Seismic Analysis Stick Model



(a) X-Direction Input

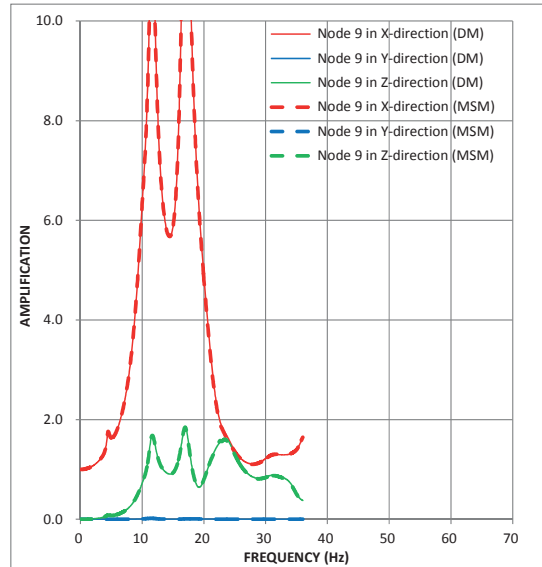


(b) Y-Direction Input

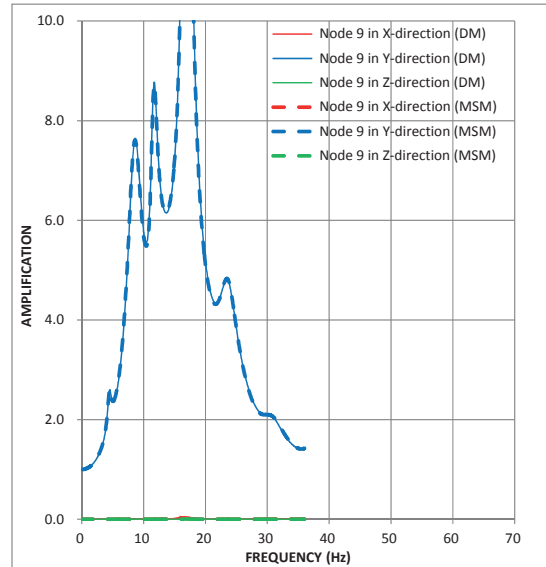


(c) Z-Direction Input

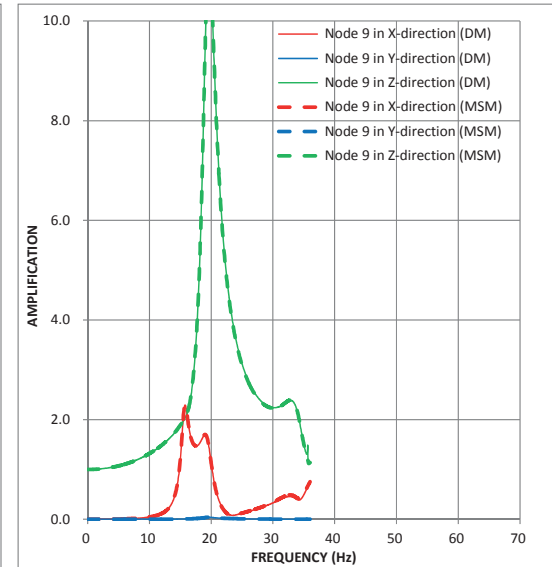
Figure 4.2-1a Comparison of Transfer Functions for FWS Wall Top Response - UB Subgrade Profile Analysis



(a) X-Direction Input

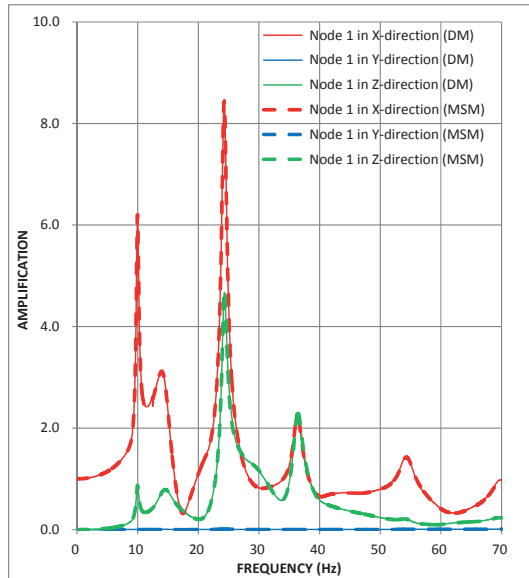


(b) Y-Direction Input

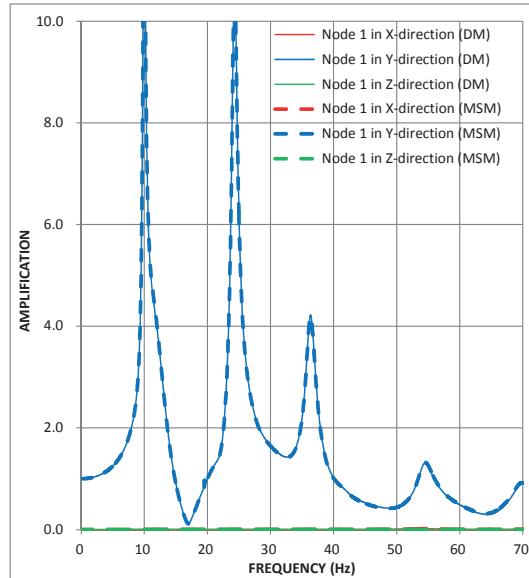


(c) Z-Direction Input

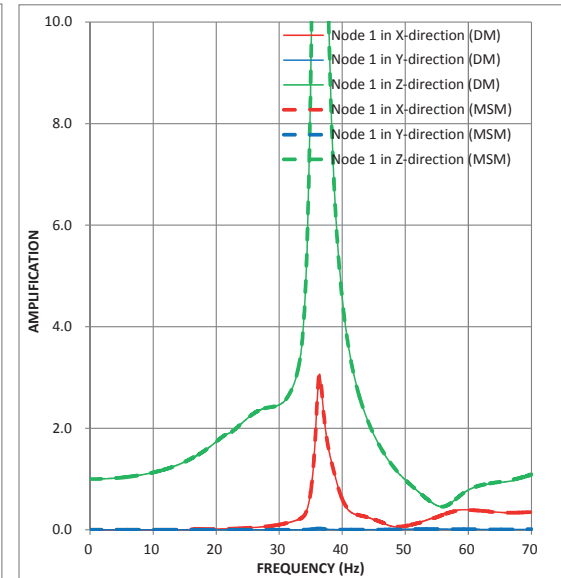
Figure 4.2-1b Comparison of Transfer Functions for FWS Wall Top Response - LB Subgrade Profile Analysis



(a) X-Direction Input

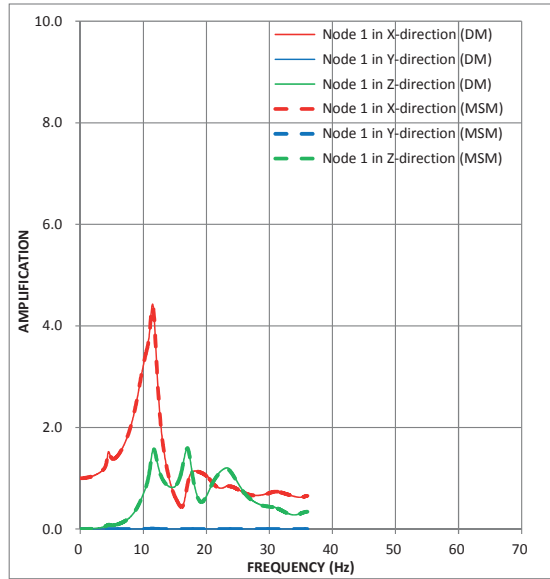


(b) Y-Direction Input

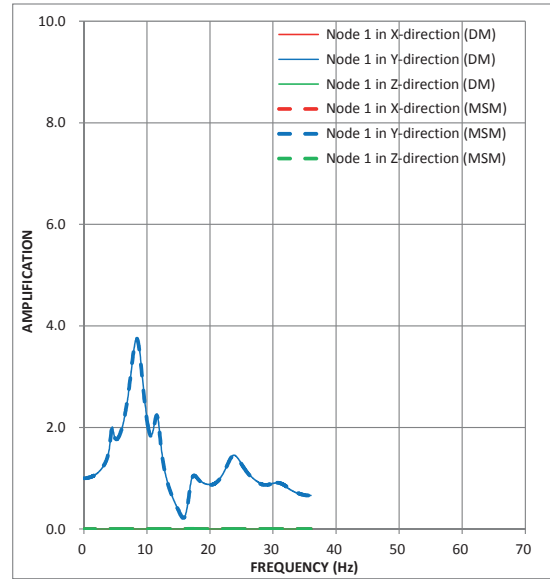


(c) Z-Direction Input

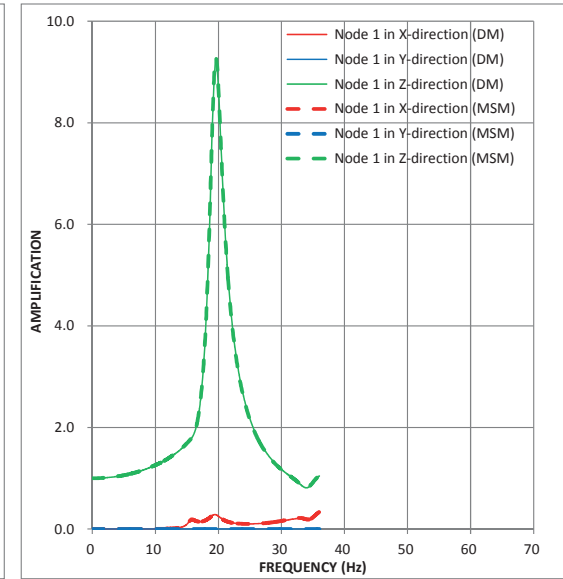
Figure 4.2-2a Comparison of Transfer Functions for FWS Basemat Response - UB Subgrade Profile Analysis



(a) X-Direction Input

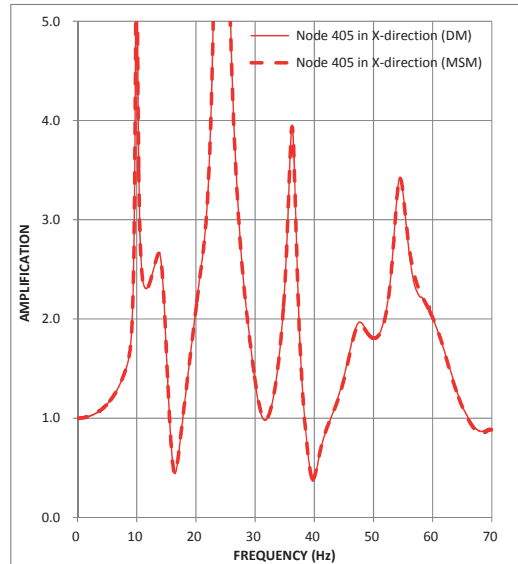


(b) Y-Direction Input

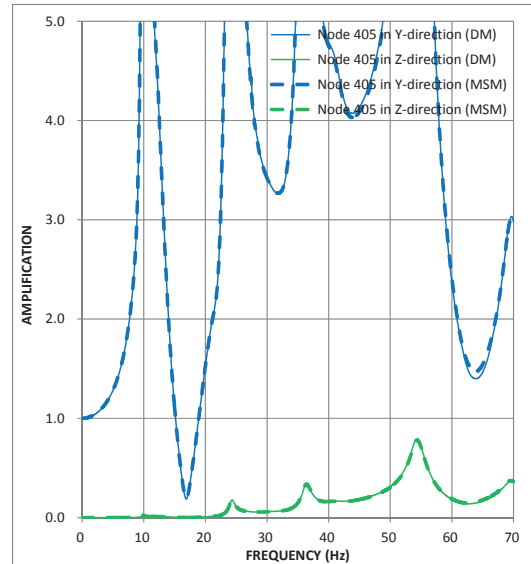


(c) Z-Direction Input

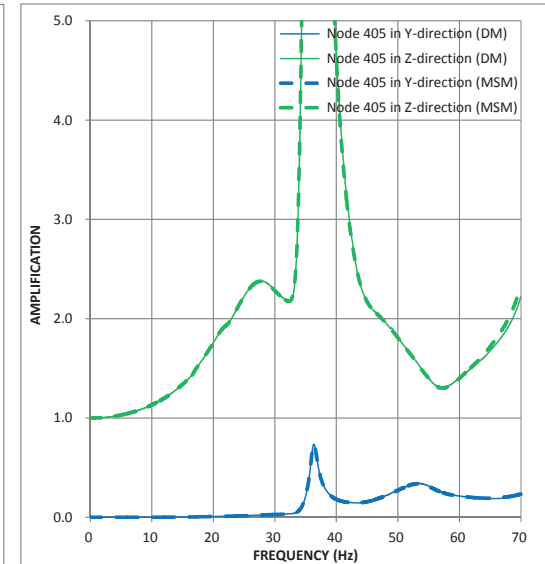
Figure 4.2-2b Comparison of Transfer Functions for FWS Basemat Response - LB Subgrade Profile Analysis



(a) X-Direction Input

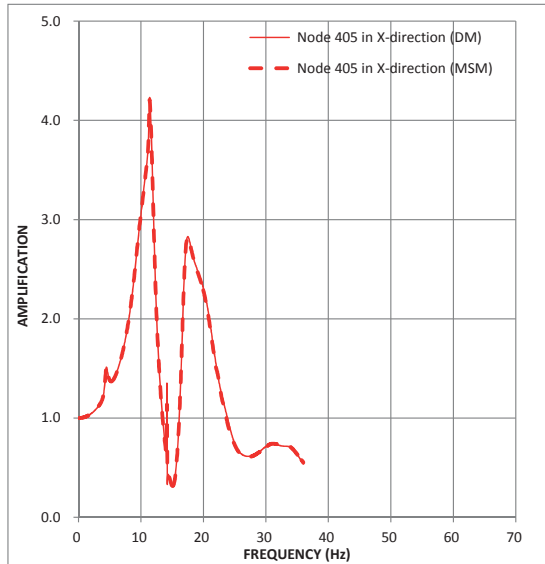


(b) Y-Direction Input

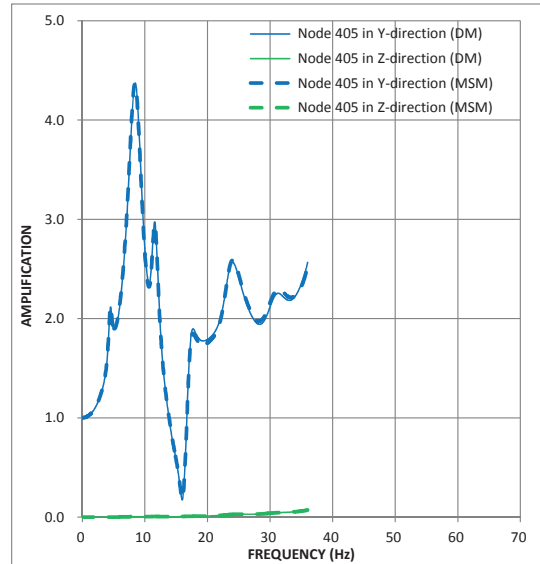


(c) Z-Direction Input

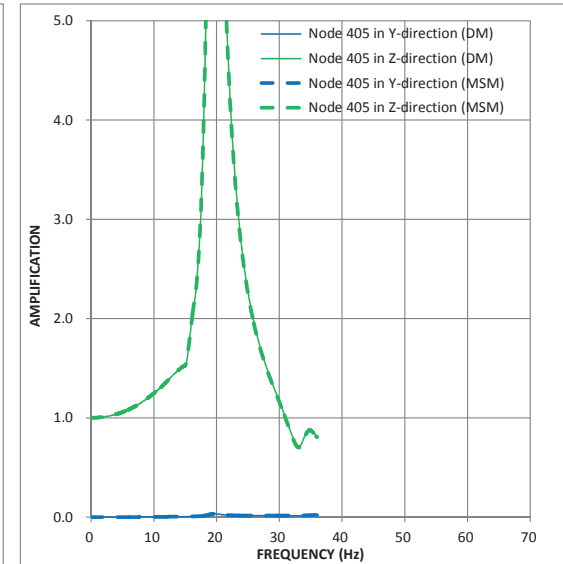
Figure 4.2-3a Comparison of Transfer Functions for FPE Top Response - UB Subgrade Profile Analysis



(a) X-Direction Input

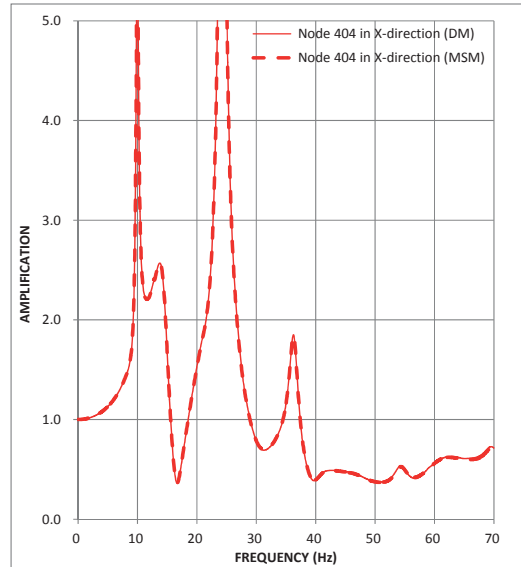


(b) Y-Direction Input

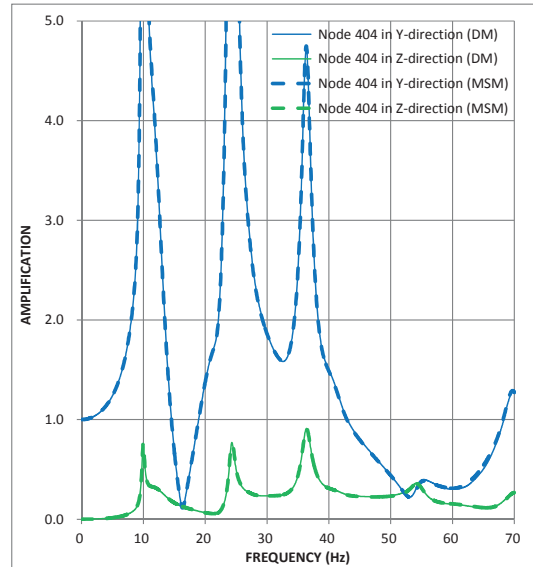


(c) Z-Direction Input

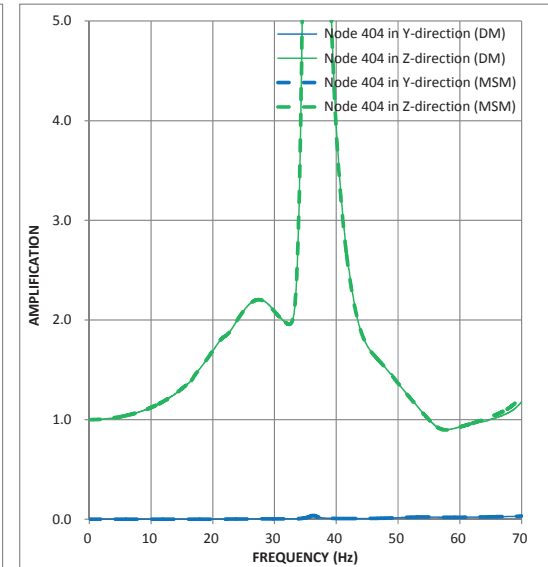
Figure 4.2-3b Comparison of Transfer Functions for FPE Top Response - LB Subgrade Profile Analysis



(a) X-Direction Input

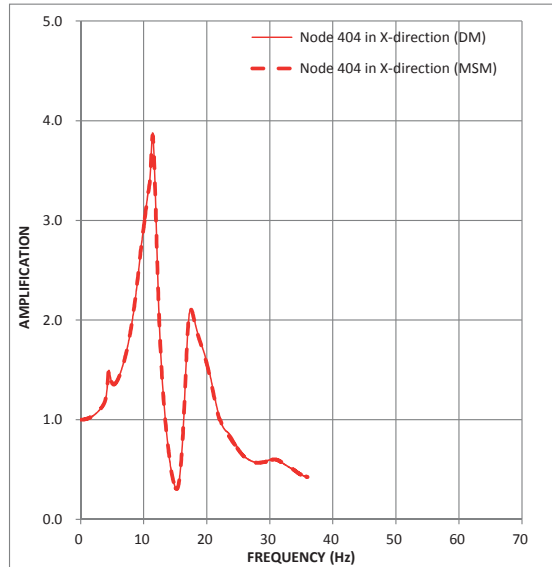


(b) Y-Direction Input

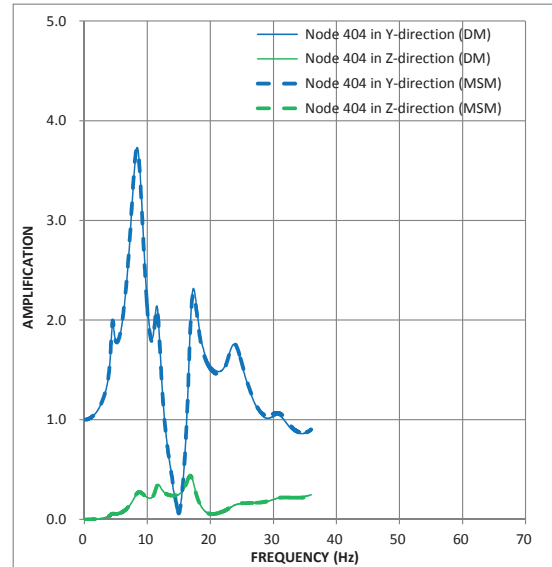


(c) Z-Direction Input

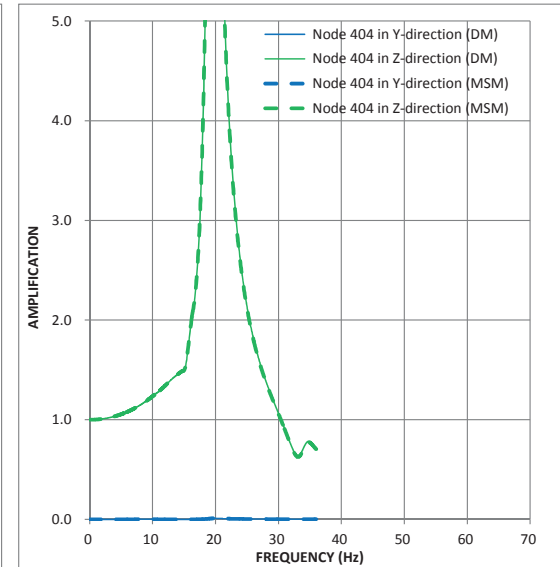
Figure 4.2-4a Comparison of Transfer Functions for FPE Basemat Response - UB Subgrade Profile Analysis



(a) X-Direction Input



(b) Y-Direction Input



(c) Z-Direction Input

Figure 4.2-4b Comparison of Transfer Functions for FPE Basemat - LB Subgrade Profile Analysis

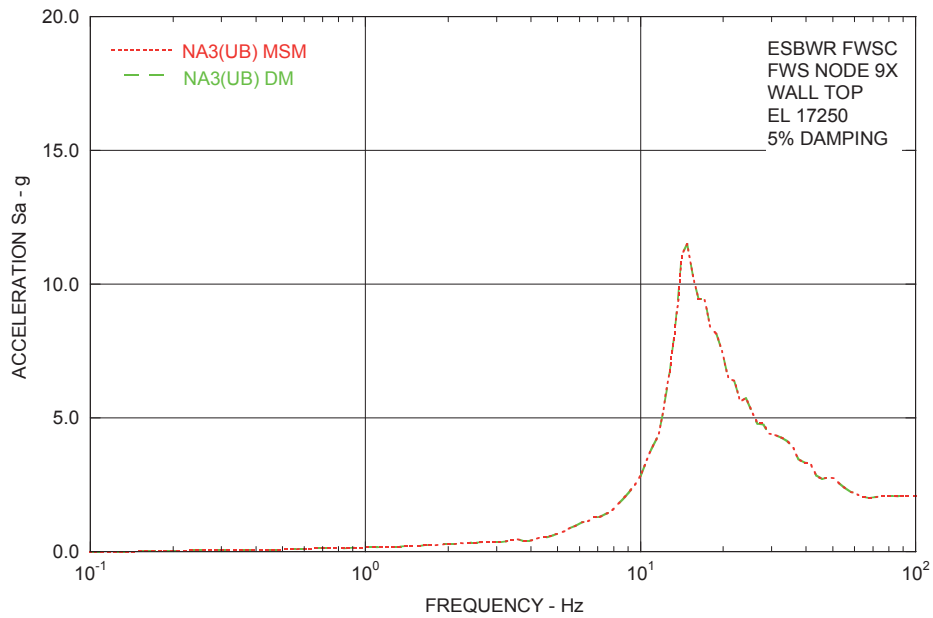


Figure 4.2-5a Comparison of ISRS for FWS Top Response in X-direction from UB Subgrade Profile Analysis

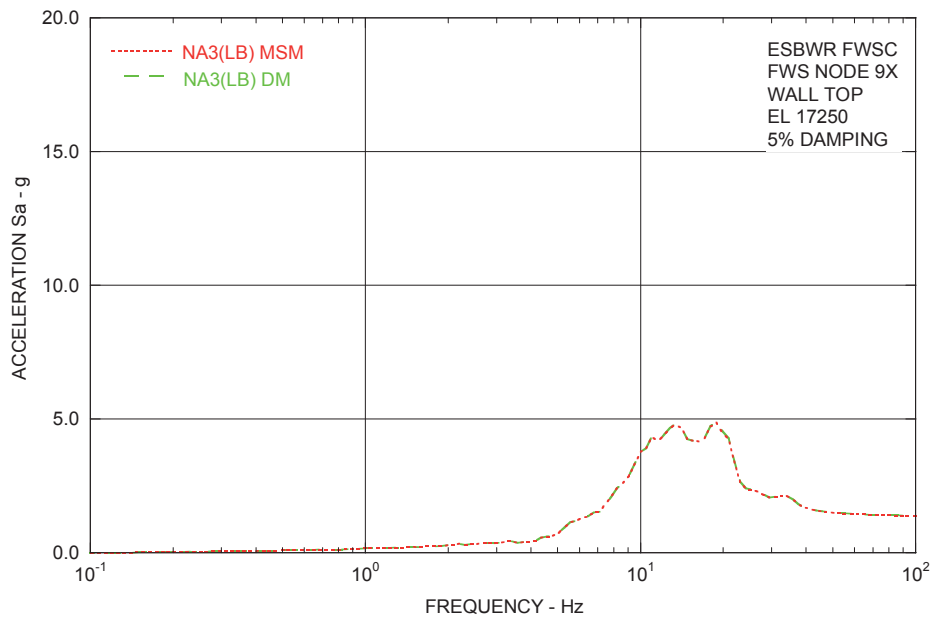


Figure 4.2-5b Comparison of ISRS for FWS Top Response in X-direction from LB Subgrade Profile Analysis

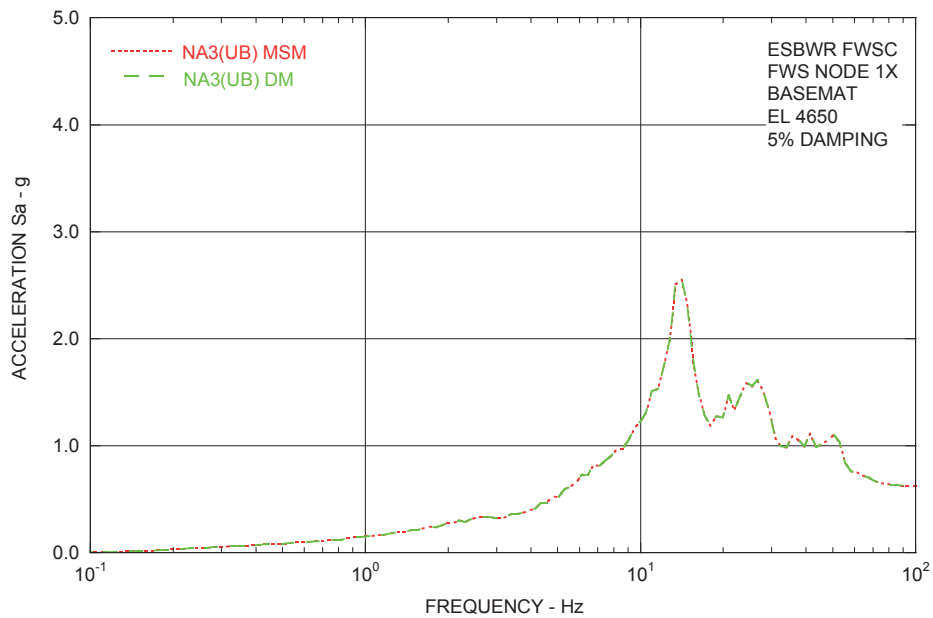


Figure 4.2-6a Comparison of ISRS for FWS Basemat Response in X-direction from UB Subgrade Profile Analysis

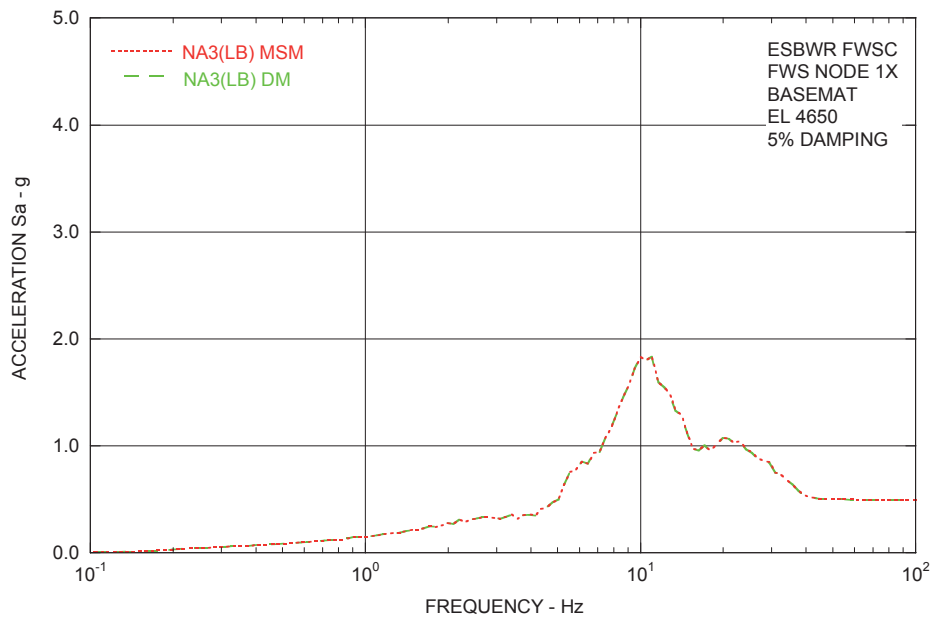


Figure 4.2-6b Comparison of ISRS for FWS Basemat Response in X-direction from LB Subgrade Profile Analysis

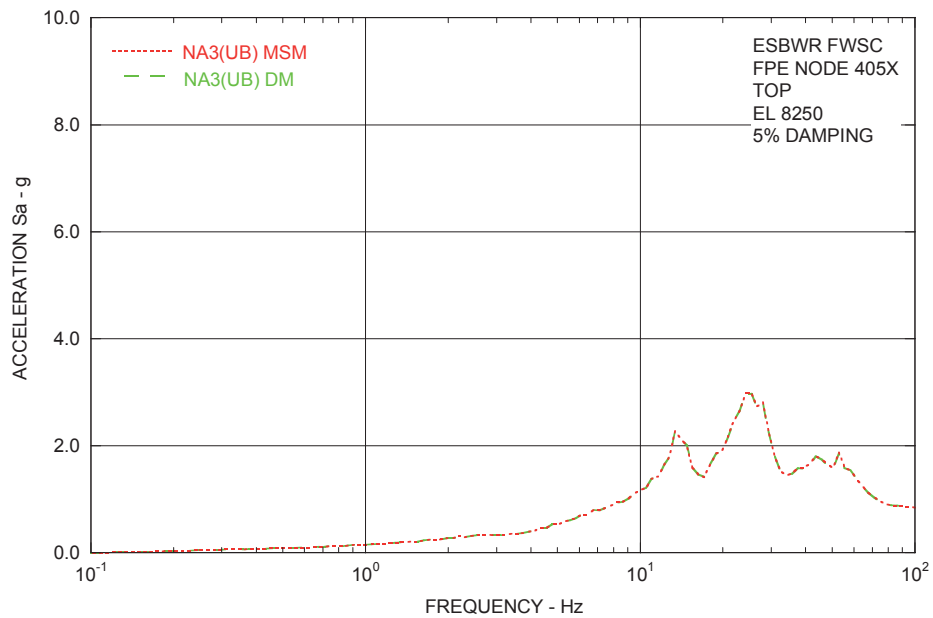


Figure 4.2-7a Comparison of ISRS for FPE Top Response in X-direction from UB Subgrade Profile Analysis

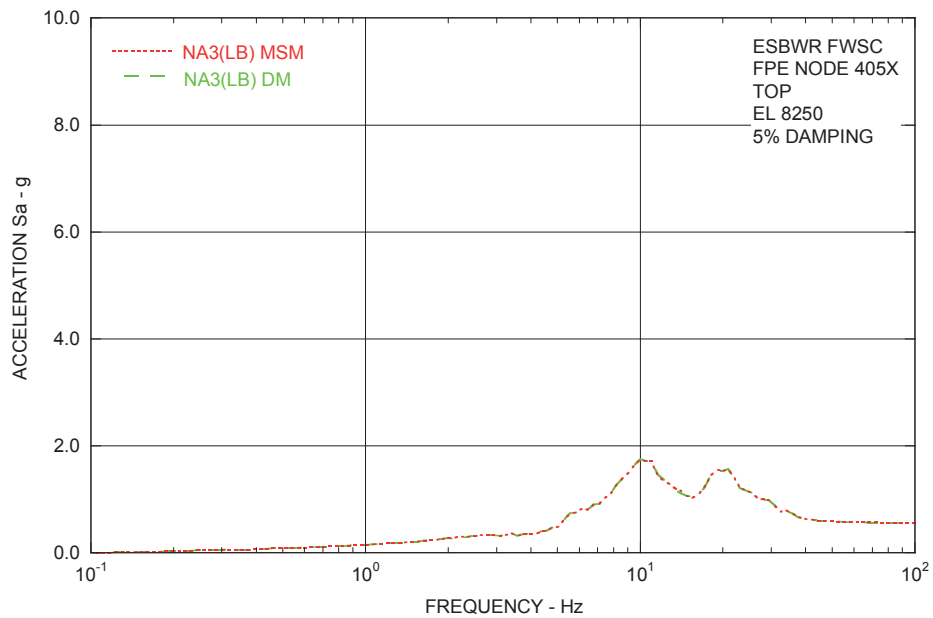


Figure 4.2-7b Comparison of ISRS for FPE Top Response in X-direction from LB Subgrade Profile Analysis

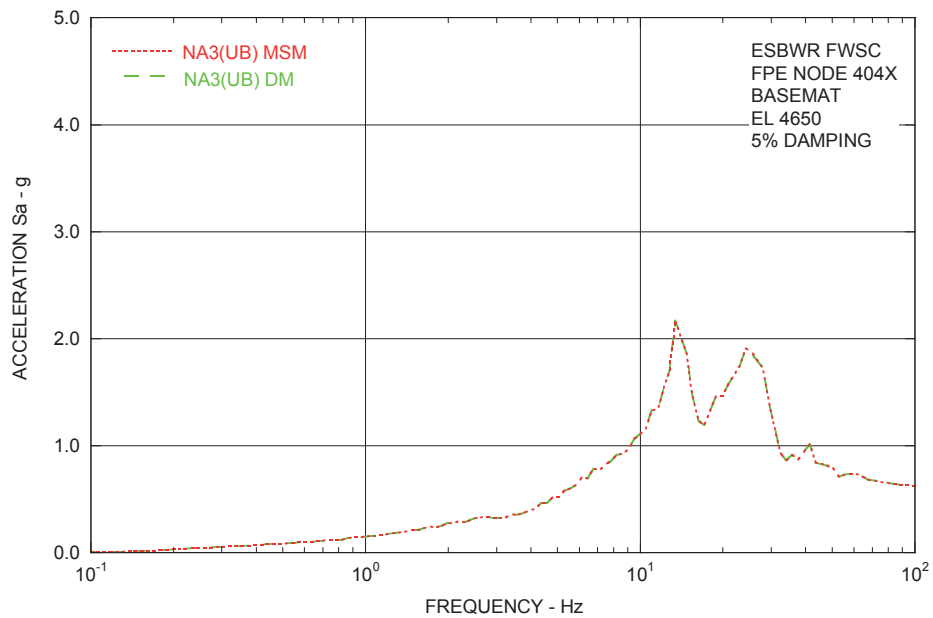


Figure 4.2-8a Comparison of ISRS for FPE Basemat Response in X-direction from UB Subgrade Profile Analysis

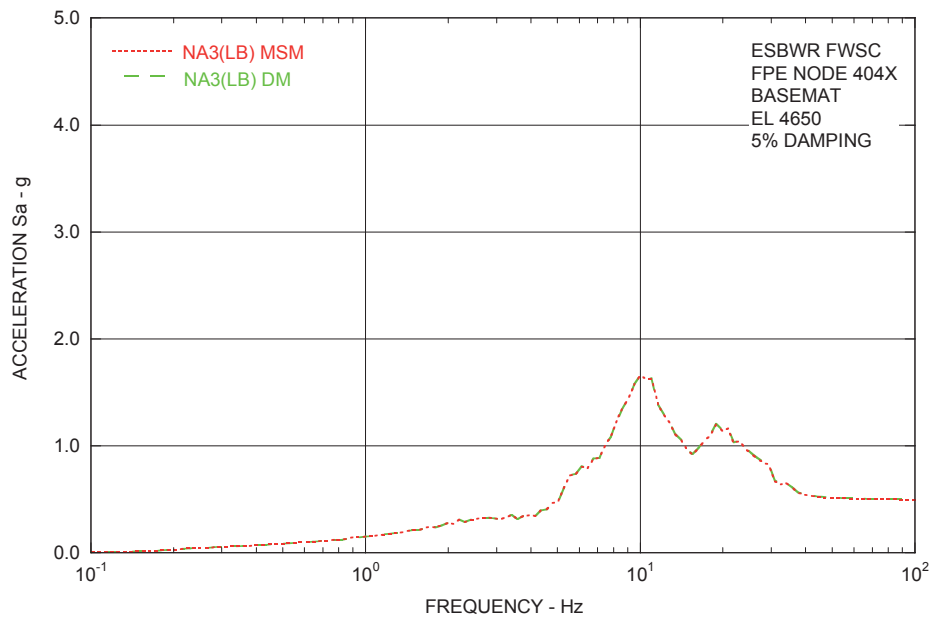


Figure 4.2-8b Comparison of ISRS for FPE Basemat Response in X-direction from LB Subgrade Profile Analysis

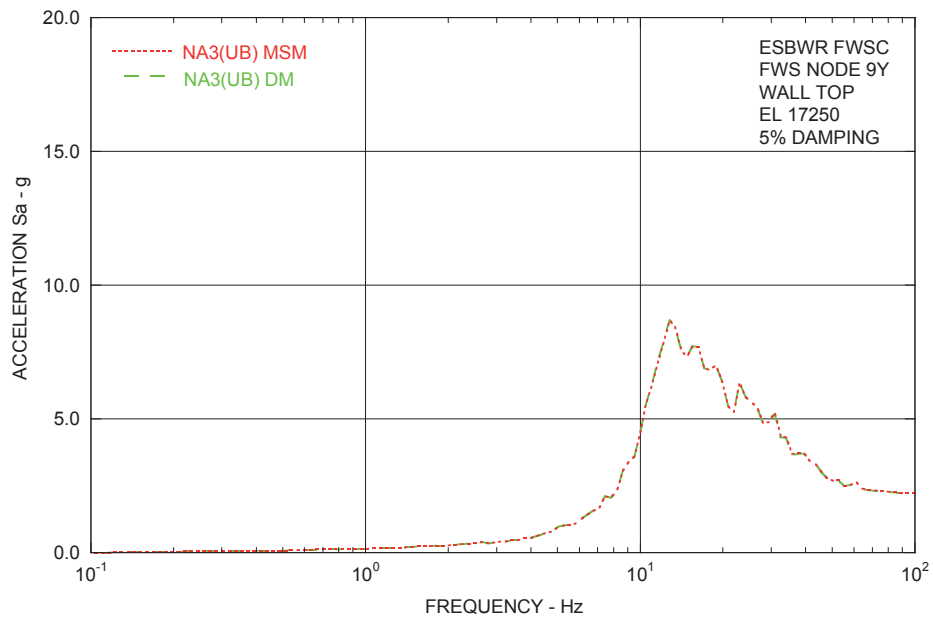


Figure 4.2-9a Comparison of ISRS for FWS Top Response in Y-direction from UB Subgrade Profile Analysis

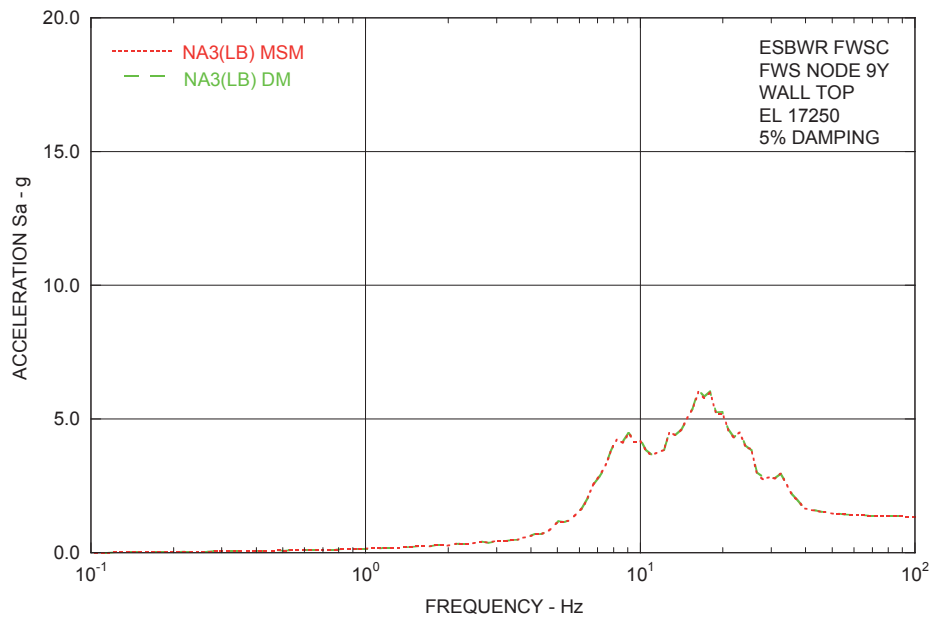


Figure 4.2-9b Comparison of ISRS for FWS Top Response in Y-direction from LB Subgrade Profile Analysis

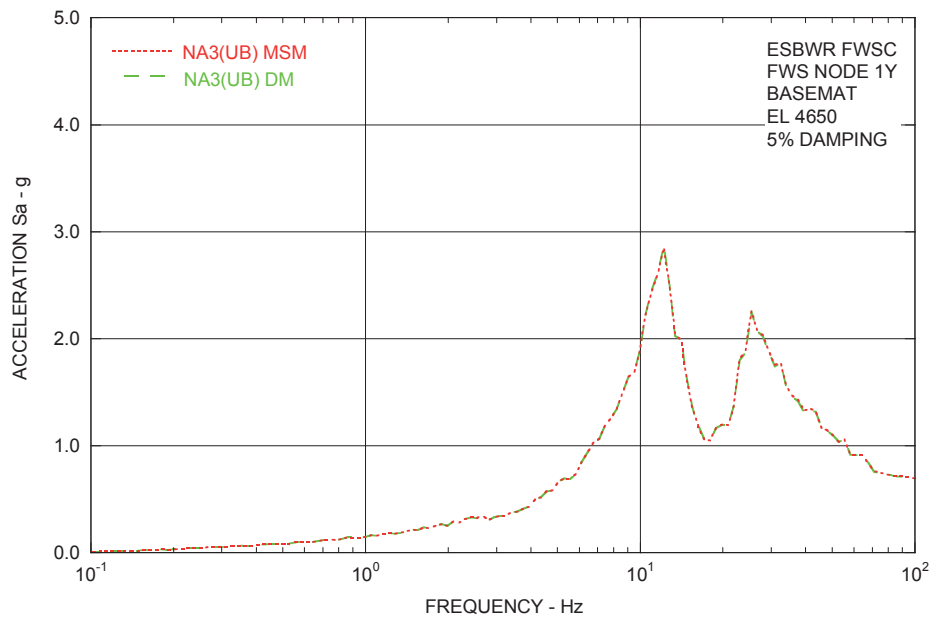


Figure 4.2-10a Comparison of ISRS for FWS Basemat Response in Y-direction from UB Subgrade Profile Analysis

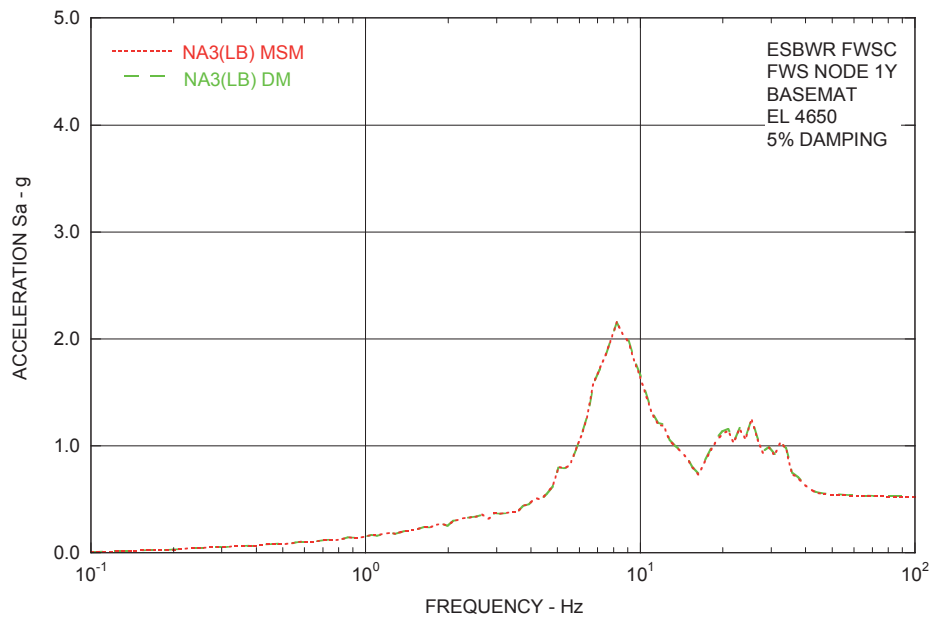


Figure 4.2-10b Comparison of ISRS for FWS Basemat Response in Y-direction from LB Subgrade Profile Analysis

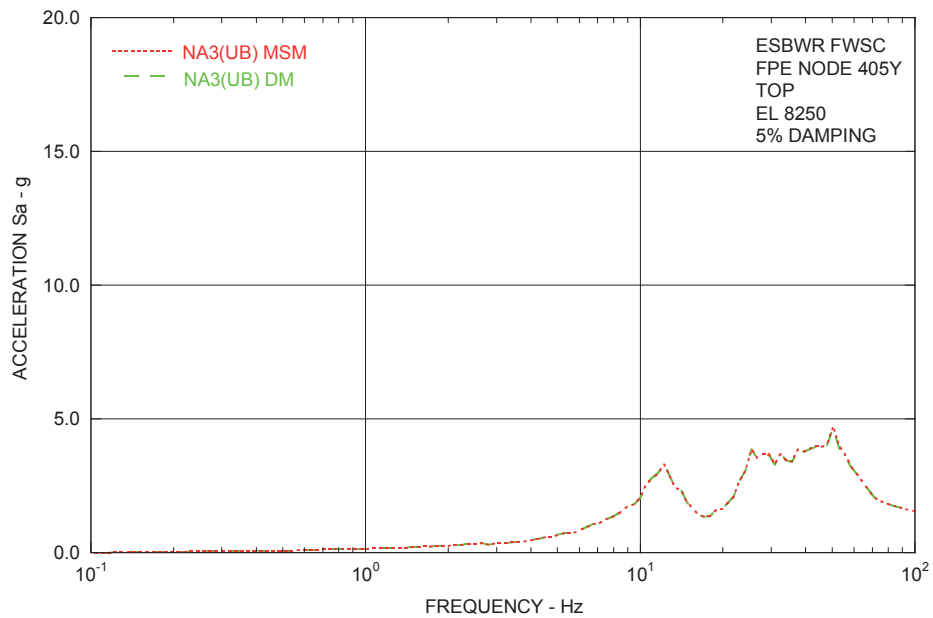


Figure 4.2-11a Comparison of ISRS for FPE Top Response in Y-direction from UB Subgrade Profile Analysis

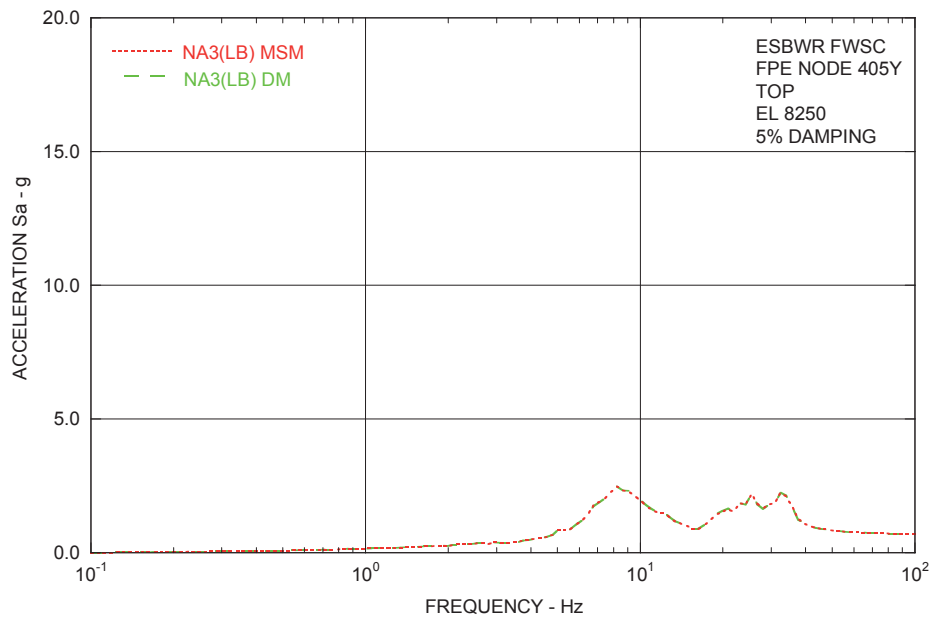


Figure 4.2-11b Comparison of ISRS for FPE Top Response in Y-direction from LB Subgrade Profile Analysis

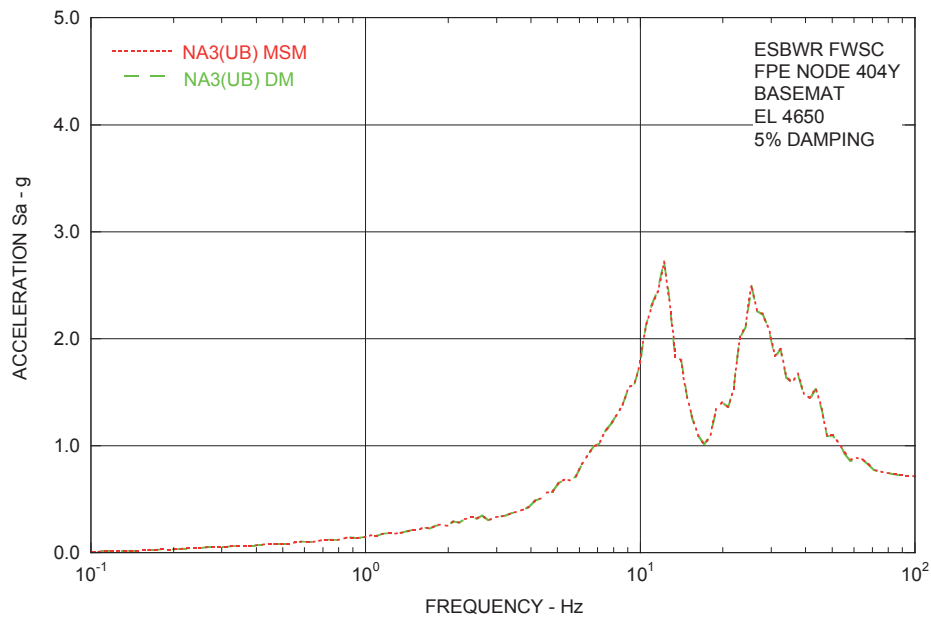


Figure 4.2-12a Comparison of ISRS for FPE Basemat Response in Y-direction from UB Subgrade Profile Analysis

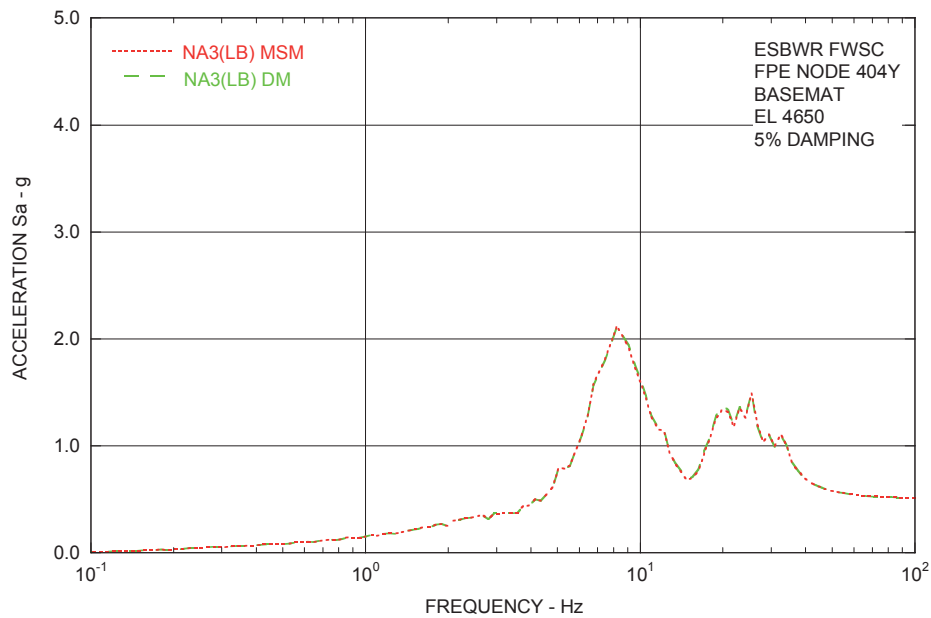


Figure 4.2-12b Comparison of ISRS for FPE Basemat Response in Y-direction from LB Subgrade Profile Analysis

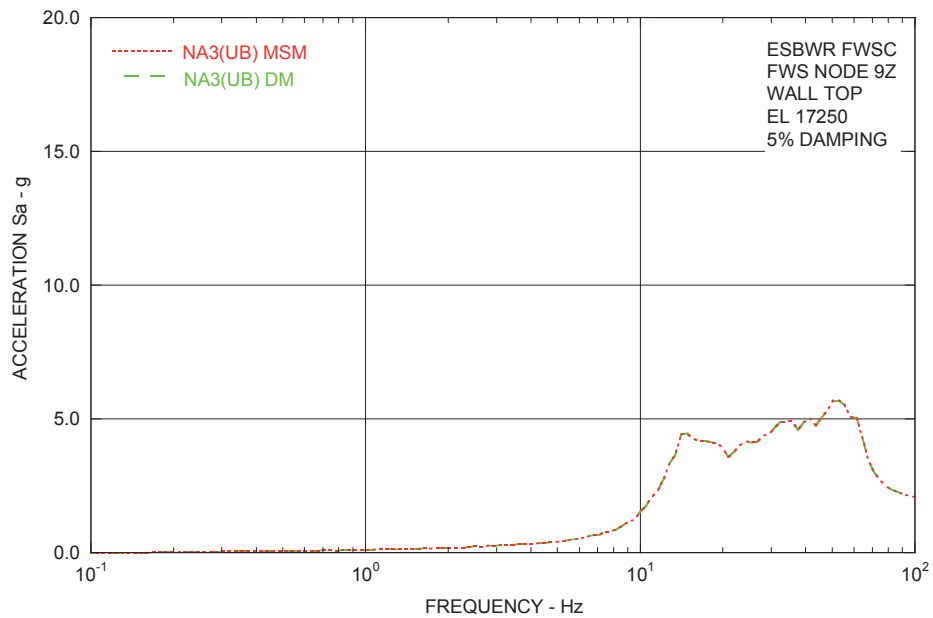


Figure 4.2-13a Comparison of ISRS for FWS Top Response in Z-direction from UB Subgrade Profile Analysis

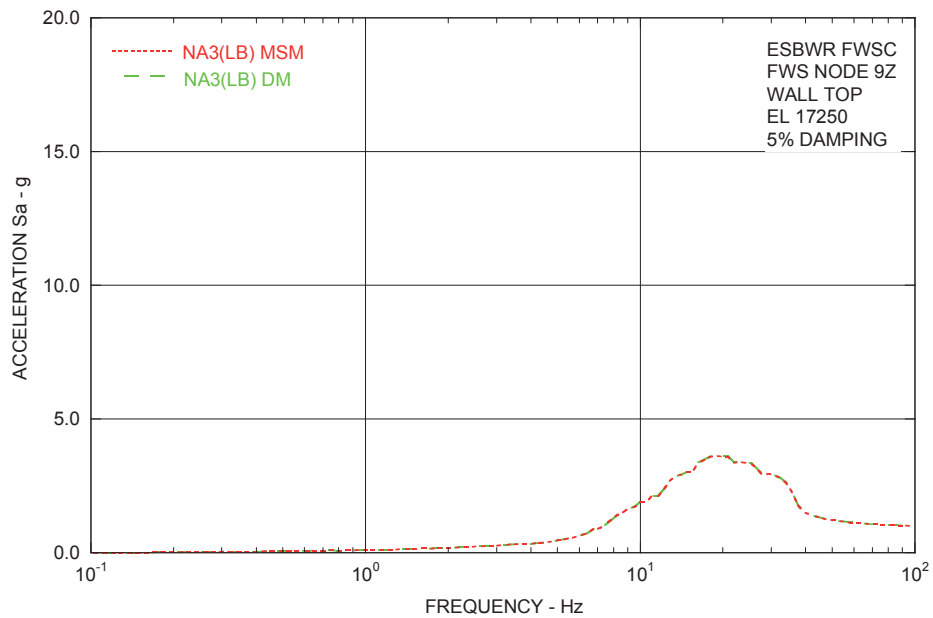


Figure 4.2-13b Comparison of ISRS for FWS Top Response in Z-direction from LB Subgrade Profile Analysis

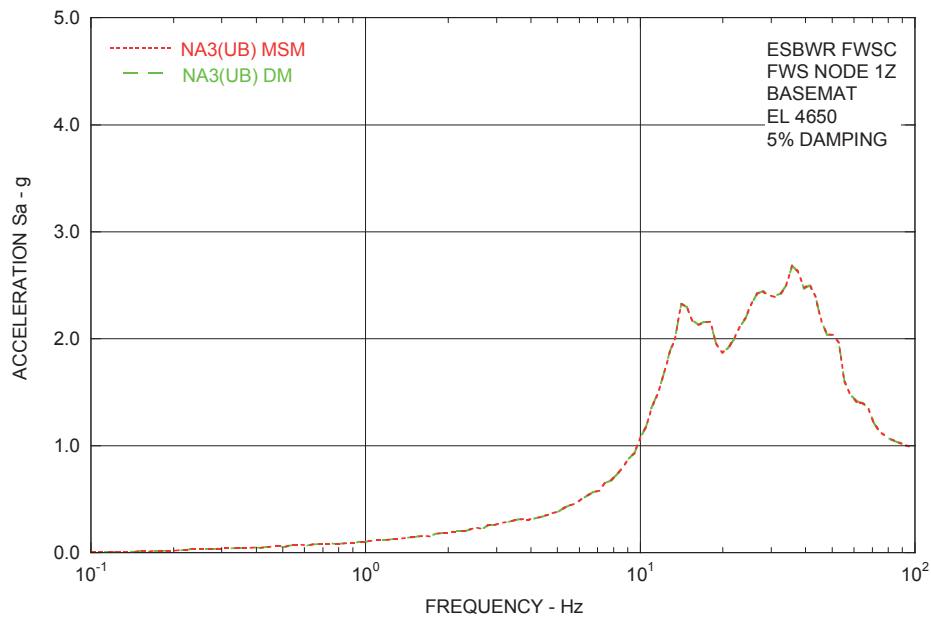


Figure 4.2-14a Comparison of ISRS for FWS Basemat Response in Z-direction from UB Subgrade Profile Analysis

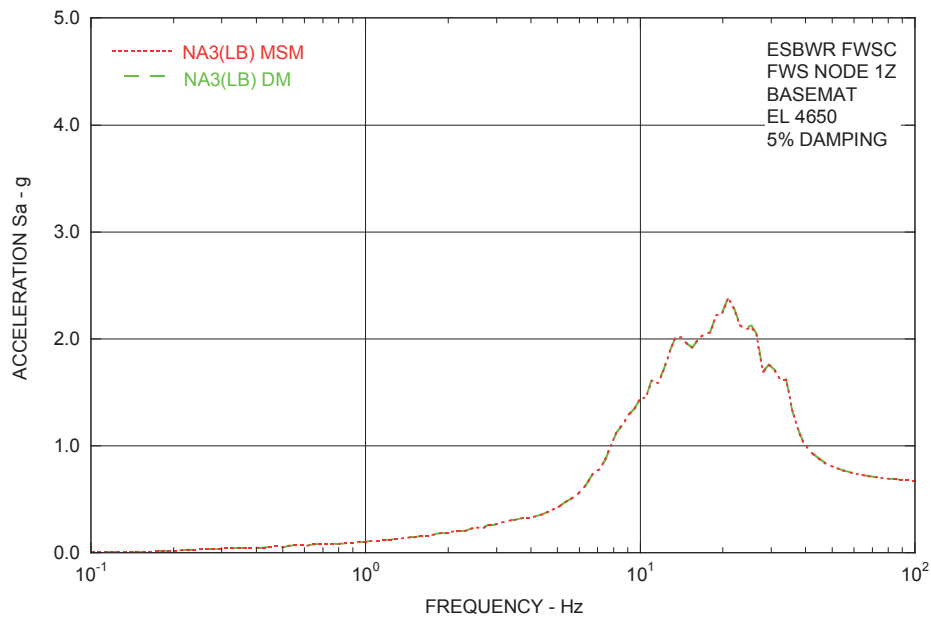


Figure 4.2-14b Comparison of ISRS for FWS Basemat Response in Z-direction from LB Subgrade Profile Analysis

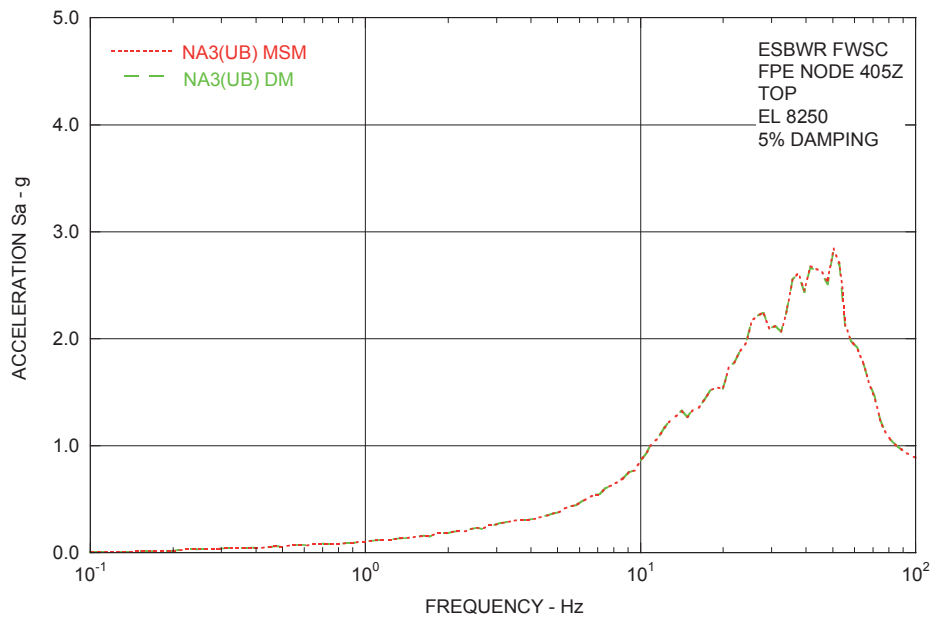


Figure 4.2-15a Comparison of ISRS for FPE Top Response in Z-direction from UB Subgrade Profile Analysis

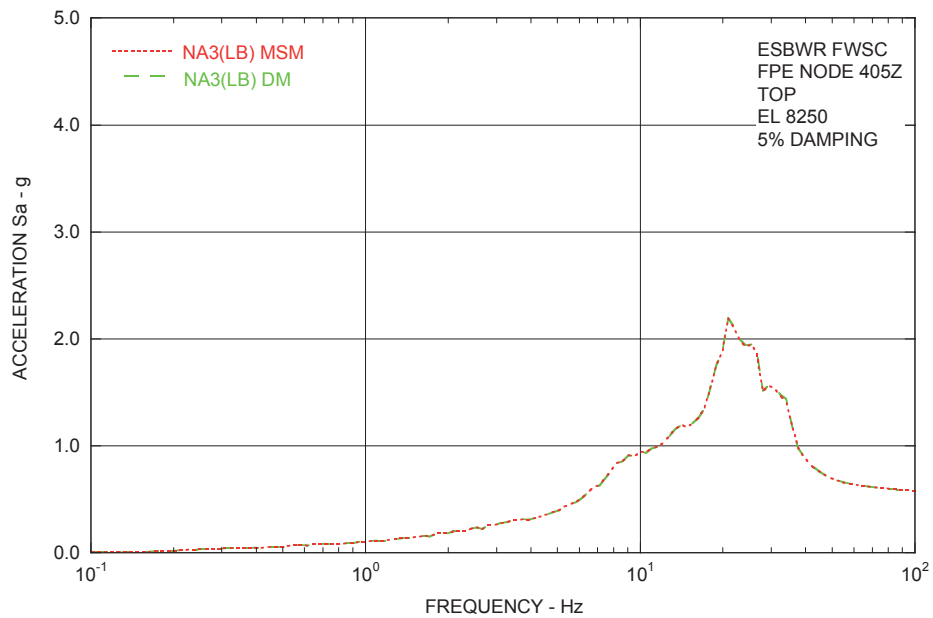


Figure 4.2-15b Comparison of ISRS for FPE Top Response in Z-direction from LB Subgrade Profile Analysis

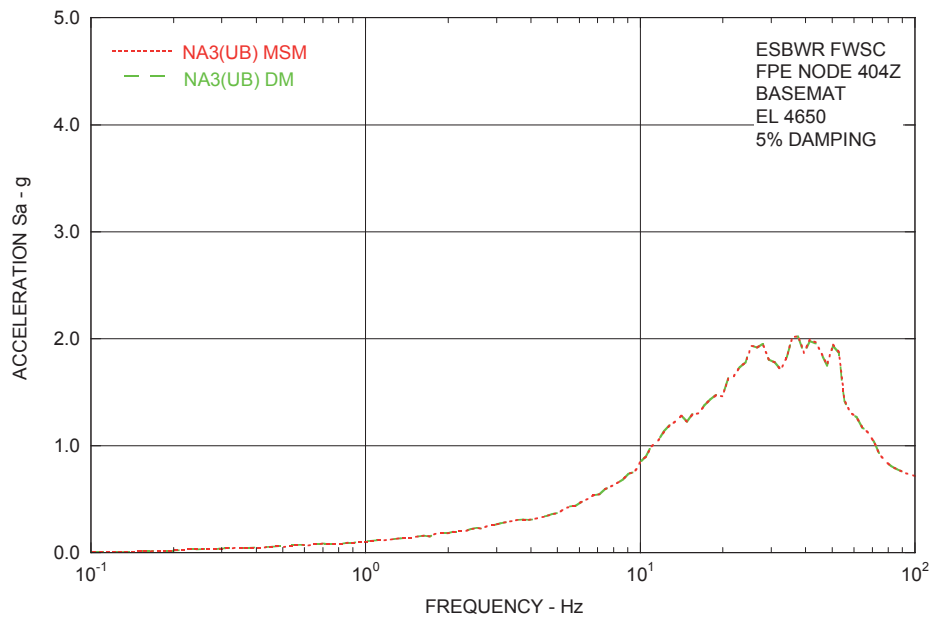


Figure 4.2-16a Comparison of ISRS for FPE Basemat Response in Z-direction from UB Subgrade Profile Analysis

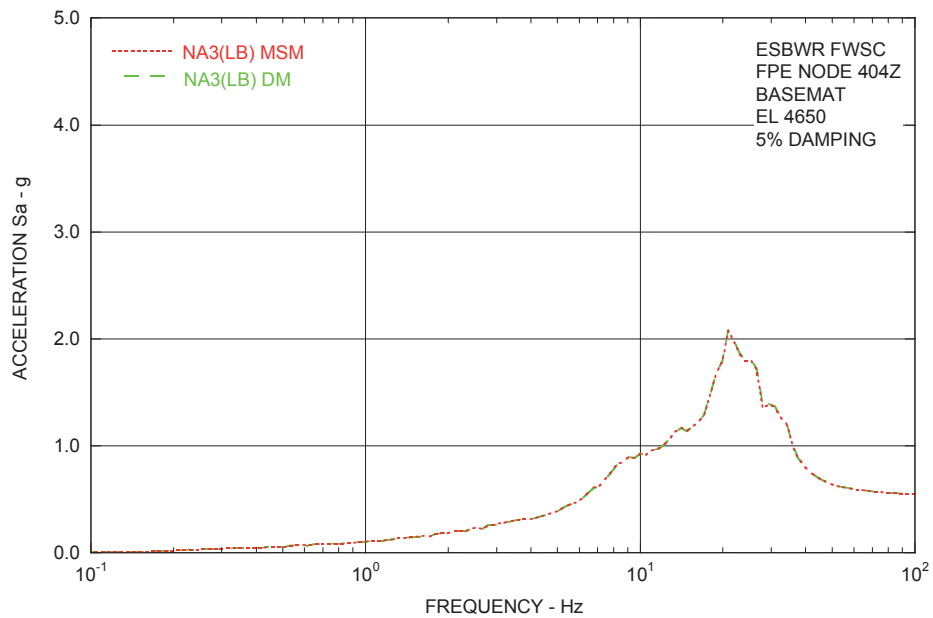


Figure 4.2-16b Comparison of ISRS for FPE Basemat Response in Z-direction from LB Subgrade Profile Analysis

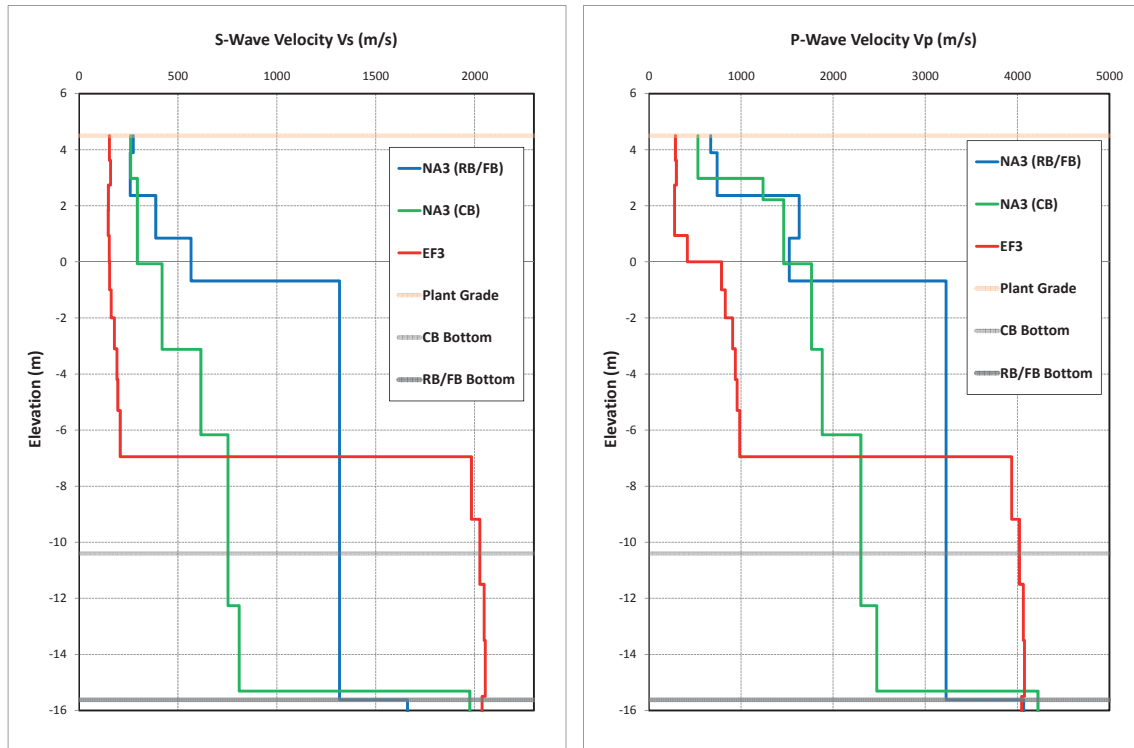


Figure 5.2-1 NA3 and EF3 S-wave and P-wave Velocity Profiles